

International Telecommunication Union



Report ITU-R BT.2407-0
(10/2017)

**Colour gamut conversion from
Recommendation ITU-R BT.2020 to
Recommendation ITU-R BT.709**

BT Series
Broadcasting service
(television)



International
Telecommunication
Union

Foreword

The role of the Radiocommunication Sector is to ensure the rational, equitable, efficient and economical use of the radio-frequency spectrum by all radiocommunication services, including satellite services, and carry out studies without limit of frequency range on the basis of which Recommendations are adopted.

The regulatory and policy functions of the Radiocommunication Sector are performed by World and Regional Radiocommunication Conferences and Radiocommunication Assemblies supported by Study Groups.

Policy on Intellectual Property Right (IPR)

ITU-R policy on IPR is described in the Common Patent Policy for ITU-T/ITU-R/ISO/IEC referenced in Annex 1 of Resolution ITU-R 1. Forms to be used for the submission of patent statements and licensing declarations by patent holders are available from <http://www.itu.int/ITU-R/go/patents/en> where the Guidelines for Implementation of the Common Patent Policy for ITU-T/ITU-R/ISO/IEC and the ITU-R patent information database can also be found.

Series of ITU-R Reports

(Also available online at <http://www.itu.int/publ/R-REP/en>)

Series	Title
BO	Satellite delivery
BR	Recording for production, archival and play-out; film for television
BS	Broadcasting service (sound)
BT	Broadcasting service (television)
F	Fixed service
M	Mobile, radiodetermination, amateur and related satellite services
P	Radiowave propagation
RA	Radio astronomy
RS	Remote sensing systems
S	Fixed-satellite service
SA	Space applications and meteorology
SF	Frequency sharing and coordination between fixed-satellite and fixed service systems
SM	Spectrum management

Note: This ITU-R Report was approved in English by the Study Group under the procedure detailed in Resolution ITU-R 1.

Electronic Publication
Geneva, 2017

© ITU 2017

All rights reserved. No part of this publication may be reproduced, by any means whatsoever, without written permission of ITU.

REPORT ITU-R BT.2407-0

Colour gamut conversion from Recommendation ITU-R BT.2020 to Recommendation ITU-R BT.709¹

(2017)

1 Introduction

In wide-gamut UHD TV production, particularly under the assumption of simultaneous live UHD TV and HDTV broadcast scenarios, real-time high-quality gamut mapping from UHD TV to HDTV is essential. This Report addresses in general the following goals:

- To advise on the advantages and disadvantages of automatic conversion techniques and to seek to identify optimum conversion mechanisms.
- To advise on any additional measures that may be appropriate in order to achieve optimum colour gamut conversion and avoiding the introduction of subjectively disturbing artefacts.
- To investigate a possible method of colorimetry conversion from Recommendation ITU-R BT.2020 (BT.2020) to Recommendation ITU-R BT.709 (BT.709) in terms of image quality and feasibility that ideally satisfies the following requirements:
 - Colours inside the BT.709 gamut should be unchanged.
 - The conversion method should facilitate multiple conversions between BT.2020 and BT.709.
 - Perceived hue change must be as small as possible.
 - No significant loss of spatial details.
 - Will not introduce visible discontinuities in colour.
 - The mapping method is mathematically definable.

There is no universal gamut mapping method which can achieve all of these requirements simultaneously. In converting from a wider colour gamut to a smaller colour gamut, modification of colours outside the BT.709 gamut is unavoidable. This conversion is necessarily a compromise between different requirements which may vary depending on the application. Gamut mapping algorithms are often motivated by aspects of artistic creation, human vision, technical constraints and experience. Metrics for identifying colour gamut conversion performance have not yet been developed along with an associated suite of tests.

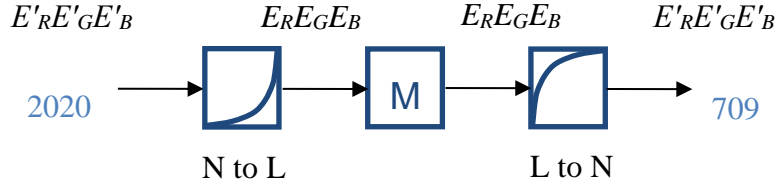
2 Simple conversion from BT.2020 to BT.709 based on linear matrix transformation

Figure 1 shows the block diagram of the colour conversion from BT.2020 to BT.709 based on linear matrix transformation. This is the exact inverse of the operation specified in Recommendation ITU-R BT.2087 for conversion from BT.709 to BT.2020, except that the output signals are hard-clipped. This method is the most straightforward and implementable in the least amount of hardware.

¹ For standard dynamic range television (SDR TV).

FIGURE 1

Colour conversion from BT.2020 to BT.709 based on linear matrix transformation



The functions and equations for each block in Fig. 1 operate as follows.

2.1 Non-linear to linear conversion (N to L)

The conversion from normalized non-linear RGB signals (E'_R E'_G E'_B) to normalized linear RGB signals (E_R E_G E_B) is calculated using one of the two non-linear to linear transfer functions specified in Recommendation ITU-R BT.2087. There are two cases described in Recommendation ITU-R BT.2087, one for the display referred approach using an electro-optical transfer function (EOTF) and one for the scene referred approach using an inverse OETF.

2.2 Matrix (M)

BT.2020 RGB signals are transformed to BT.709 RGB signals using the following equations:

$$\begin{aligned}
 \begin{bmatrix} E_R \\ E_G \\ E_B \end{bmatrix}_{709} &= \begin{bmatrix} 0.4124 & 0.3576 & 0.1805 \\ 0.2126 & 0.7152 & 0.0722 \\ 0.0193 & 0.1192 & 0.9505 \end{bmatrix}^{-1} \begin{bmatrix} 0.6370 & 0.1446 & 0.1689 \\ 0.2627 & 0.6780 & 0.0593 \\ 0 & 0.0281 & 1.0610 \end{bmatrix} \begin{bmatrix} E_R \\ E_G \\ E_B \end{bmatrix}_{2020} \\
 &= \begin{bmatrix} 3.2410 & -1.5374 & -0.4986 \\ -0.9692 & 1.8760 & 0.0416 \\ 0.0556 & -0.2040 & 1.0570 \end{bmatrix} \begin{bmatrix} 0.6370 & 0.1446 & 0.1689 \\ 0.2627 & 0.6780 & 0.0593 \\ 0 & 0.0281 & 1.0610 \end{bmatrix} \begin{bmatrix} E_R \\ E_G \\ E_B \end{bmatrix}_{2020} \\
 &= \begin{bmatrix} 1.6605 & -0.5876 & -0.0728 \\ -0.1246 & 1.1329 & -0.0083 \\ -0.0182 & -0.1006 & 1.1187 \end{bmatrix} \begin{bmatrix} E_R \\ E_G \\ E_B \end{bmatrix}_{2020} \tag{1}
 \end{aligned}$$

NOTE – All values in the above matrices were calculated with high precision and then rounded to four decimal digits.

2.3 Linear to non-linear conversion (L to N)

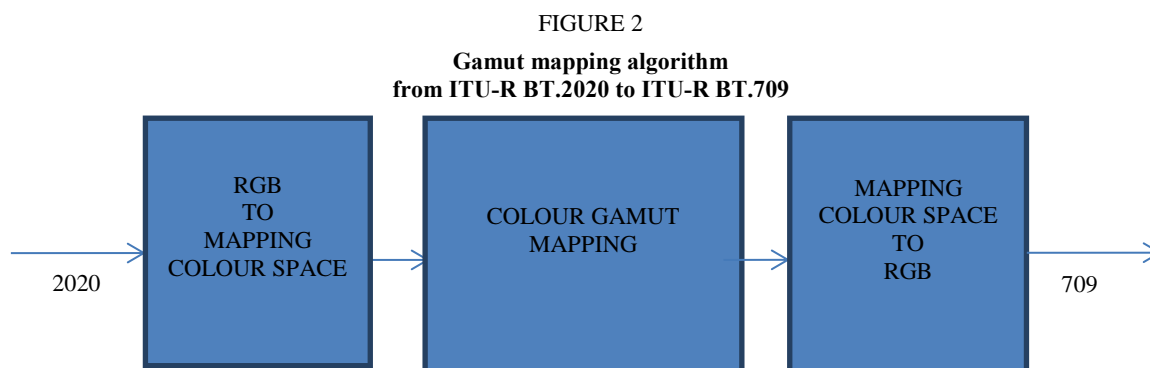
The conversion from normalized linear RGB signals (E_R E_G E_B) to normalized non-linear RGB signals (E'_R E'_G E'_B) is calculated using one of the two linear to non-linear transfer functions specified in Recommendation ITU-R BT.2087. There are two cases described in Recommendation ITU-R BT.2087, one for the display referred approach using an inverse EOTF and one for the scene referred approach using an OETF.

2.4 Practical limitations

This method has the very desirable property that it does not alter colours within the BT.709 gamut, even after multiple conversions between BT.2020 and BT.709. However, colours outside the BT.709 gamut are hard-clipped, i.e. RGB signals (E_R E_G E_B) that are less than zero or greater than one are clipped to zero or one, which can lead to significant hue shifts and loss of spatial detail. Most content will look just fine, but these artefacts can conflict with the requirements for hue and spatial detail preservation.

3 Principles of gamut mapping

To improve upon the results of simple linear matrix transformation with hard-clipping, a well-designed gamut mapping process may be performed. Figure 2 shows a diagram of a general gamut mapping algorithm from BT.2020 to BT.709. The input BT.2020 RGB signals are converted to the coordinates of a selected mapping colour space, then the colours within the ITU-R BT.2020 colour gamut are mapped to colours within the BT.709 colour gamut based on a gamut mapping algorithm. The gamut-mapped colours are then converted to the output BT.709 RGB signals.



The selection of mapping colour space is a crucial aspect to conversion.

Some of the different mapping colour spaces that may be used are:

- CIE xyY
- CIE u'v'Y
- CIE L*a*b*
- Simplified Lab
- Uniform colour space based on CIECAM02

In the CIE xyY and u'v'Y colour spaces, linear colour mixing holds. BT.2020 or BT.709 RGB (E_R E_G E_B) values can be linearly converted to the CIE xyY and u'v'Y coordinates by simple linear and projective operators. The xy plane is the traditional representation of chromaticity², while the u'v' chromaticity plane has the advantage of being perceptually more uniform than the xy plane when Y is constant.

When using xyY or u'v'Y mapping colour spaces, designing gamut mapping algorithms can be expected to be simpler by utilizing linear transforms. However, if a mapping path –used to map a colour from BT.2020 colour gamut to BT.709 colour gamut– is straight, perceived lightness, chroma and hue of colours may change simultaneously.

² Chromaticity is a representation of the ratio of each set of three tristimulus coordinates values to their sum.
NOTE 1 – As the sum of the three chromaticity coordinates equals 1, two of them are sufficient to define a chromaticity.

NOTE 2 – In the CIE standard colorimetric systems, the chromaticity coordinates are represented by the symbols x, y, z and x10, y10, z10.

NOTE 3 – Definition reference is 845-03-33 in CIE Publication Number 17.4.

NOTE 4 – Chromaticity values are typically specified as xy pairs, though other chromaticity pairs such as u'v', which is a mathematical transform of xy, are also in common use.

The CIE L*a*b* colour space was designed to have a better visual uniformity than xyY or u'v'Y colour spaces. The Simplified Lab colour space is a simplification of the CIE L*a*b* colour space in which colour gamuts have simpler shapes with approximately plane surfaces. The CIE L*a*b* and simplified Lab colour spaces require more complex, non-linear operations to derive them from BT.2020 or BT.709 (E_R E_G E_B) values. One advantage of these colour spaces is their perceptual uniformity that takes lightness into account; Euclidean distances in the three-dimensional colour space are nominally proportional to the perceived colour differences. Another advantage is that the colour spaces have the cylindrical coordinates L*C*h* or simplified L_sC_sh_s corresponding to perceptual lightness, chroma, and hue, respectively. If a source colour is mapped to a target colour having the same metric hue angle h or h_s, the perceived hue can be expected to be the same.

When using CIE L*a*b* or simplified Lab colour spaces, linear mapping paths may preserve one or two of lightness, chroma, and hue. Along these mapping paths, source colours from BT.2020 are moved to BT.709 target colours. This modification of colours may involve linear or non-linear functions.

CIECAM02 established by CIE Technical Committee 1-34 has an advantage in the prediction of blue hue. The significant non-uniformity of the CIE L*a*b* metric blue hue is improved.

Some gamut mapping methods preserve all of the colours inside the BT.709 gamut while the other methods modify some colours within the BT.709 gamut, especially those near the BT.709 gamut boundary. This modification of colours within the BT.709 colour gamut can cause significant artefacts when multiple round trip conversions are performed.

It should be noted that through the use of metadata or content analysis, the content colour gamut, defined as the actual distribution of colours in a programme or scene, may be determined. Since the content colour gamut is often much smaller than the total BT.2020 colour gamut, the amount of required colour gamut compression is reduced with an accompanying reduction in distortions. Note that this additional information is not dependent on a specific algorithm, i.e. the result of any algorithm could be improved by using content colour gamut.

4 Conclusion

Many techniques exist to perform gamut mapping, utilizing many different combinations of the tools described above. It has proven impossible to select just one method as the single, best option for performing BT.2020 to BT.709 video conversions. The six Annexes to this Report detail some examples of advanced gamut mapping systems, and are included as background information to help readers in their understanding of what kinds of options may be available in the industry. Table 1 is provided to help compare the design goals and characteristics of the mapping methods found in the Annexes. The presence or absence of a specific feature should not be interpreted as an indicator of overall quality of any mapping method, but simply illustrates the different choices that were made when developing these assorted methods. Definitions for the column headings are as follows:

Functional Simplicity: Was the mapping method deliberately constructed using only simple functional elements, such as low complexity colour space conversions, low complexity mapping techniques, or other simplified characteristics? Note that functional simplicity does not necessarily impact implementation complexity as all of these mapping methods would likely utilize a 3D look up table in hardware, thereby eliminating any complexity differences in implementation.

Colour Appearance Space: Within which colour appearance space is the gamut mapping performed?

Hue Mapping: Does the mapping method modify hues of colours?

Lightness Mapping: Does the mapping method modify lightness of colours?

Parametric Construction: Is the mapping method constructed using a design that contains adjustable parameters which allow tuning of the mapping details?

Reversible Operation: Is the mapping potentially method reversible, such that though an inverse operation, the original BT.2020 image may be fully reconstructed from the BT.709 mapped result?

Roundtrip Possible with BT.2087: Is the mapping method constructed such that multiple roundtrips with BT.2087 will not lead to continuously degrading content (after the initial limiting to the BT.709 gamut)?

Considers Content Colour Gamut: Can the mapping method take advantage of knowledge that the content does not fill the entire BT.2020 gamut? This knowledge could come through analysis, from metadata provided by the source, or by design of the algorithm.

TABLE 1

Mapping Method Annex	Functional Simplicity	Colour Appearance Space	Hue Mapping	Lightness Mapping	Parametric Construction	Reversible Operation	Roundtrip Possible with BT.2087	Considers Content Colour Gamut
1	No	CIELAB	Yes	Yes	No	Yes	No	No
2	No	CIELAB	Yes	Yes	No	No	Yes	No
3	Yes	Simplified CIELAB	Yes	Yes	Yes	No	No	No
4	No	CIELAB or Modified CIECAM02	Yes	Yes	Yes	Yes	No	Yes
5	Yes	Yu'v'	No	No	Yes	Yes	No	No
6	No	CIELAB	Yes	Yes	No	Yes	No	Yes

References

- [1] *Photography and graphic technology – Extended colour encodings for digital image storage, manipulation and interchange – Part 1: Architecture and requirements*, ISO 22028-1.

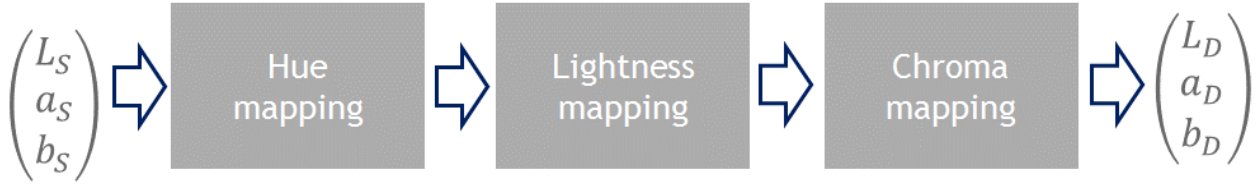
Annex 1

Figure A1-1 shows a block diagram for a modular method for mapping hue, lightness and chroma of colours within Recommendation ITU-R BT.2020 in order to move them into Recommendation ITU-R BT.709. The mapping method consists of the following three steps:

- 1 Hue mapping;
- 2 Lightness Mapping;
- 3 Chroma mapping.

FIGURE A1-1

Modular lightness, hue and chroma mapping from BT.2020 to BT.709



The following sections present the three steps of the modular mapping method.

A1.1 Hue mapping

Hue h is the angle defined by a colour projected into the a^*b^* -plane. Hue is an aspect of colour that should generally be preserved during conversion. However, misalignment of hues of primary and secondary colours may lead to suboptimal behaviour of succeeding steps of colour gamut mapping.

In fact, non-uniform saturation modifications may occur when the primary colours defining the source colour gamut and the primary colours defining the target colour gamut are significantly mismatched.

The modular method aims to improve the uniformity of the saturation modification induced by colour gamut mapping, notably to minimize the degradation of colour neighbourhood while minimizing the average change of hue. The modular method includes thus a hue mapping method that adaptively changes the source hue of a source primary colour towards the target hue of the corresponding target primary colour based on the difference in hue and chroma of the source and target primary colours.

When comparing the colour gamuts of BT.2020 and BT.709, notably the green primaries are misaligned:

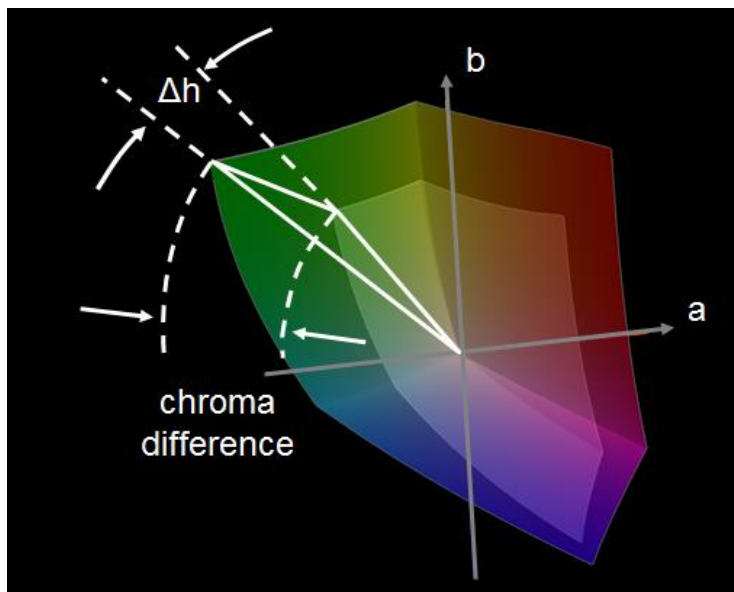
	Recommendation ITU-R BT.2020 (source)		Recommendation ITU-R BT.709 (target)			
	Hue h_S	Chroma C_S^*	Hue h_T	Chroma C_T^*	Δh	$\Delta \alpha$
Red primary	40.58°	154.49	40.00°	104.55	−0.58°	177.0°
Green primary	145.91°	208.07	136.01°	119.78	−9.9°	144.3°
Blue primary	305.60°	147.92	306.29°	133.81	0.69°	166.3°

Hue h and chroma c^* are derived from $L^*a^*b^*$ colour space. L^*C^*h build a cylindrical coordinate system. The c^* axis represents chroma. It lies in the a^*b^* plane and goes from the centre of this plane ($a^*=b^*=0$) where colours have low saturation or low chroma ($C^*=0$) to large values of a^*, b^* where colours have large saturation or large chroma (large C^*). The h^* axis represents hue. Hue h is the angle formed by the C^* axis and the a^* axis. Hue goes from red ($h=0$) via yellow and green to blue and then again to red.

For each source primary colour, the hue change is applied to make the saturation difference from the corresponding target primary colour smaller. Figure A1-2 shows a triangle formed by the origin and the projections in the a^*b^* plane of the source and target green primary colours. One angle of the triangle is the hue difference Δh . The difference $\Delta \alpha = 144.3^\circ$ of the two other angles of the triangle expresses geometrically the difference of saturation of the green primary colours. A practical hue change that increases with decreasing $\Delta \alpha$ can be according to: $h \cos \frac{\Delta \alpha}{2}$. The described hue mapping applies therefore a rotation of hue in CIELAB space of $-9.9^\circ \cos \frac{144.3^\circ}{2} = -3$ degrees for the green primary. For the red and blue primary colours, the applied rotation of hue is 0.0° and 0.1° , respectively.

FIGURE A1-2

Hue difference Δh and chroma difference between the green primaries of the source colour gamut BT.2020 (large gamut) and the target colour gamut BT.709 (small gamut) as well as the triangle formed by the green primaries and the origin (white line)



A1.2 Lightness mapping

Lightness is an aspect of colour that should be modified very carefully during conversion in order to avoid unwanted change of brightness and contrast. However, misalignment of the lightness of colours from source and target gamuts may lead to suboptimal behaviour of succeeding steps of colour gamut mapping. Therefore, the modular mapping method includes a lightness mapping method. This lightness mapping method is controlled by the cusp lines and by the rims of the source and the target colour gamuts. The cusp line of a colour gamut is a line joining cusp colours, wherein a cusp colour is a colour of maximum chroma in the constant-hue leaf of the source colour to be mapped. The rims of a colour gamut correspond to the ridges of the colour gamut linking the white point to the secondary colours and to the ridges linking the black point to the primary colours.

A cusp line is calculated such that its projection on a plane of constant lightness (for example the *ab*-plane of CIELAB space) is the smallest convex polygon enclosing the colour gamut projected in this same plane. In the described lightness mapping, when the source and/or the target colour gamut is non-convex in CIELAB colour space, the described cusp line of such a colour gamut might have a cusp colour that is located out of colour gamut in a constant-hue leaf.

The described lightness mapping method operates within a constant-hue leaf and is based on the following well-known idea: A colour in a hue leaf having the lightness and the chroma of a cusp colour of the source colour gamut is lightness mapped to a colour having the same lightness as a cusp colour of the target colour. A corresponding lightness mapping function is defined, linearly propagated to and finally applied to the source colour.

The described lightness mapping is enhanced to cope with two issues. One issue in lightness mapping is that generally a colour gamut in CIELAB space is curved. The curvature of a colour gamut generally reflects the curvature of the CIELAB colour space. For this reason, there is generally a mismatch between the linear propagation of the described mapping function and the curvature of the colour gamuts. A solution is to get a representation of the curvature in hue-direction at the location of colours belonging to the hue leaf of the source colour inside the source and target colour gamut, respectively.

The described lightness mapping method uses therefore a lightness mapping function that depends on the lightness values of other source and target cusp colours of constant-hue leaves different from the hue leaf of the source colour to be mapped. For example, the average of lightnesses of these other source or target cusp colours, respectively, might be used to define a robust lightness mapping function. Additionally, source and target cusp colours have generally not the same hue as the source colour to be mapped. For example, the source cusp colour is simply defined to be an intersection of the source cusp line with the plane defined in BT.2020 E_R, E_G, E_B colour space by the source colour to map, by the white point and by the black point of BT.2020.

Lightness mapping is advantageous notably for saturated colours close to the cusp. For example, the green primary of the source gamut has a larger lightness than the green primary of the target colour gamut. The described lightness mapping therefor reduces the lightness of all colours such that the chroma of colours close to the green primary are better preserved during the following chroma mapping. However, a second issue in lightness mapping is that – in relation with the example of the green primary – green colours with low lightness are hereby driven farer away from the target colour gamut and will lose chroma during the following chroma mapping. Therefore, the described lightness mapping applies an additional lightness mapping step that distributes more colours into the target colour gamut by mapping the colours in opposite direction compared to the main lightness mapping.

A1.3 Chroma mapping

The modular mapping method includes a chroma mapping algorithm that maps colours along straight mapping paths that are anchored each to an anchor point belonging to the achromatic L-axis.

The mapping paths are chosen such that the variation of the gradients of the mapping paths along a curve intersecting the paths is continues and smooth (continuity of first derivation). This ensures smooth mapping and preservation of colour neighbourhood.

Each source colour is mapped onto a target colour in direction to the above defined anchor point along the mapping trajectory. The mapping of a source colour can be described as a modification of the distance D of this source colour from the anchor point into a distance D' of the target colour from the same anchor point.

In order to map D to D' , the three-segment mapping function [1] is used having

- a first segment having a slope of one covering 40% of the source chroma,
- a last segment being a hard clipping,
- and a middle segment connecting the other two segments covering 60% of chroma.

The resulting colour is expressed in CIE 1976 ($L_D \ a_D \ b_D$) coordinates.

A1.4 Practical remarks

The modular mapping method includes three partial gamut mapping steps each applying a geometrical transformation in colour space. An input colour is successively processed using these three successive colour gamut mapping steps. Each of the three steps is determined with respect to the gamut boundaries. For example, the first geometric transform is determined based on the gamut boundary of the source colour gamut relative to the gamut boundary of the target colour gamut. The second geometric transform is determined based on an intermediate colour gamut relative to the target gamut boundary. This intermediate colour gamut is determined by applying the geometrical transformation of the first step to the source colour gamut. In the same way, the third geometric transform is determined based on a second intermediate colour gamut relative to the target gamut boundary. This second intermediate colour gamut is determined by applying the geometrical transformation of the second step to the first intermediate colour gamut.

In order to generate the results of these experiments, a 3D LUT is calculated (resolution $33 \times 33 \times 33$) for the conversion method according to Fig. 2 using the modular mapping method.

A1.5 Experimental results

Figure A1-3 shows BT.2020 test pictures encoded in BT.2020 R',G',B' coordinates and intended for a BT.2020 display.

Figure A1-4 shows the test pictures processed using the simple method based on linear matrices (a) and using the modular (3DLUT) method (b). 3DLUT size is $65 \times 65 \times 65$. All images are shown in BT.709 R, G, B coordinates and are not adapted in any way to any proof view scenario.

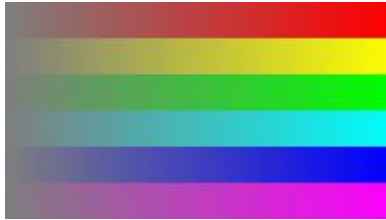
Both colour conversion methods allow to reproduce the majority of colours in quite acceptable way. But in case of linear matrices method, we lose in some cases spatial details, transparency and hue precision. This can be clearly seen in Fig. A1-4. Spatial details on the pink ball at bottom (3b) and on the flowers (4b) are better preserved. Fog transparency and pink hues are better preserved (5b) while some colour differences in pinks (6a) are destroyed by the linear matrices method since the colours out of BT.709 gamut are clipped to the gamut boundary. The saturation of the red circle on the bottle (7a) and the orange patches at right bottom (7a) is higher for the linear matrices method thanks to clipping, while the hue of these colours is better preserved (7b) by the modular method.

Given results were calculated using display referred linear/nonlinear conversions and narrow range signals.

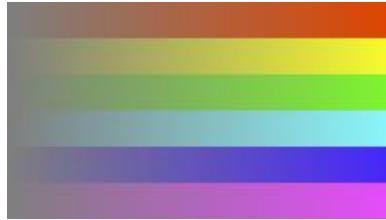
FIGURE A1-3

Test images encoded in BT.2020 R',G',B' coordinates:

- (a) colour transitions from grey to BT.2020 primary and secondary colours,
- (b) colour transitions from grey to DCI P3 primary and secondary colours,
- (c) fruits image produced within DCI P3 colour gamut,
- (d) poppy image produced within BT.2020 colour gamut,
- (e) pink scene image produced within BT.2020 colour gamut,
- (f) pink patches image produced within BT.2020 colour gamut,
- (g) glas image produced within BT.2020 colour gamut



(a)



(b)



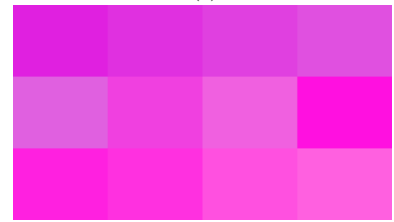
(c)



(d)



(e)



(f)

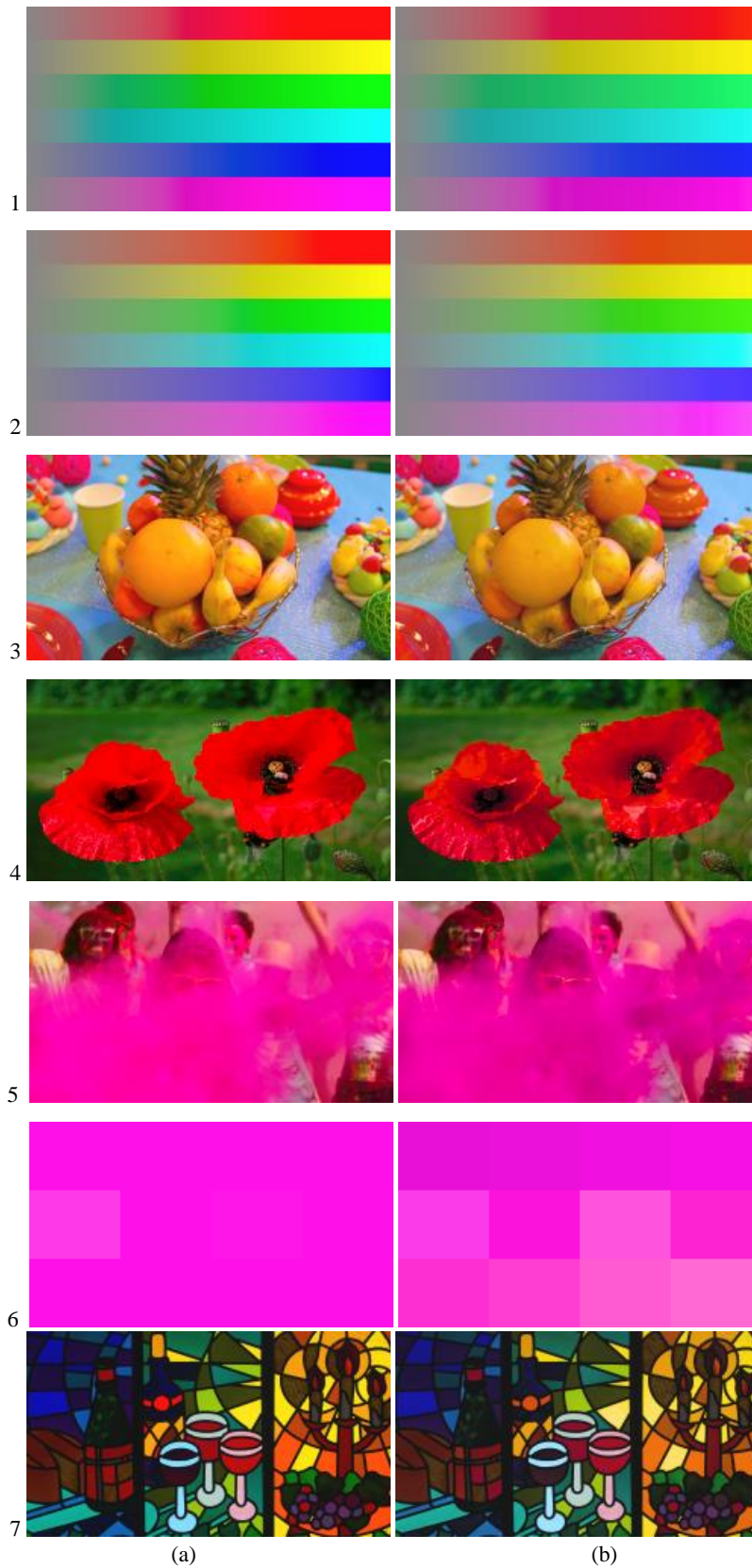


(g)

The modular conversion method based on a 3D LUT keeps better details, transparency and hue, as opposed to the linear matrices method.

FIGURE A1-4

Processed test images using (a) linear matrix transformation and (b) modular method (3D LUT)



A1.6 Conclusion

In this Annex 1 is described a conversion method to convert BT.2020 content into legacy BT.709 content according to Fig. 2 using the modular mapping method. The modular method is based on colour gamut mapping in CIELAB space. This modular method has been compared to a straightforward method which is based on EOTF and linear matrices. The results demonstrates that the modular conversion method preserves spatial details, transparency and hue of colours out of BT.709 gamut while the straightforward method shows for some images significant loss in image quality.

References

- [1] E.D. Montag, M.D. Fairchild, C.F. Carlson, Gamut mapping: Evaluation of chroma clipping techniques for three destination gamuts, IS&T/SID Sixth Color Imaging Conference, Scottsdale.

Annex 2

In this Annex 2, a combined hue, lightness and chroma gamut mapping algorithm [1] is described.

A2.1 Selection of colour appearance model

In general, the operation of a gamut mapping algorithm is based on the specific relationships between the respective appearance attributes of the source and destination. Most gamut mapping techniques are intended to retain the perceived hue of the source as predicted by a colour appearance model [2]. The latest colour appearance model, CIECAM02 [3], is believed to be the most accurate in predicting the appearance attributes, and is thought to be suitable for gamut mapping [2]. However, it has been reported that gamut mapping from wide-gamut digital cinema using CIECAM02 results in a significant hue discontinuity in the blue region [4]. One of the reasons for this is that even the latest colour appearance model fails to predict the appearance attributes of saturated colours outside the psychophysical data from which the model was derived [5]. It was showed that two modern colour appearance models, IPT [6] and CIECAM02, have significant artefacts in their hue prediction in the blue region outside the BT.709 gamut [7]. It was then decided to design our gamut mapping algorithm based on the relatively simple CIE 1976 $L^*a^*b^*$ (CIELAB) colour model with certain modifications when necessary.

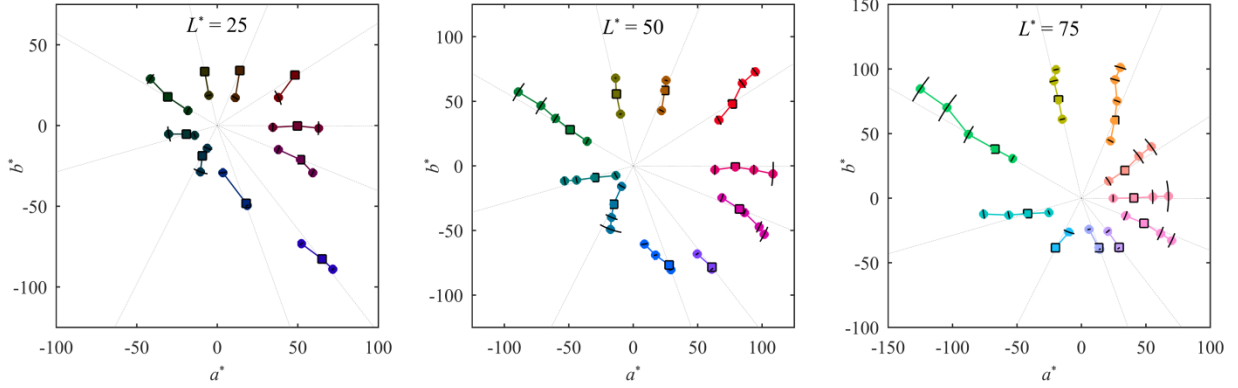
A2.2 Constant perceived hue in Recommendation ITU-R BT.2020 gamut

To ascertain the constant perceived hues inside the BT.2020 gamut, we measured them using our laser projector [8]. Twenty-five observers conducted a matching task involving ten hue angles at three lightness values in the CIELAB colour space. A reference colour patch on the BT.709 gamut surface and a test colour patch inside or outside the BT.709 gamut with the same lightness but a different chroma were presented side-by-side using a 20% gray background surrounded by a white border. The observers controlled the hue angle of the test patch to make the perceived hue the same as that of the reference patch. Figure A2-1 shows the mean values of the constant perceived hue angles with standard deviations. Significantly erroneous hue predictions were found in the blue and cyan hues in the CIELAB colour space. Although CIELAB has a well-known limitation in the discrepancies between the perceived and predicted blue hues [6, 9], the gap between the BT.2020 and BT.709 gamuts in the blue region is small, and this inaccurate prediction of the CIELAB metric hue is insignificant and rather beneficial for gamut mapping from BT.2020 to BT.709 because the BT.2020

blue primary was designed to have the same CIELAB metric hue as the BT.709 blue primary [10, 7], which prevents significant chroma loss in a hue-preserved gamut mapping. Regarding cyan hues, cyan on the BT.709 gamut boundary consistently appears slightly greenish when compared with cyan outside the BT.709 gamut with the same CIELAB metric hue angle.

FIGURE A2-1

Mean values of constant perceived hue angles with standard deviations ($N=25$)



(Square markers show the reference colours.)

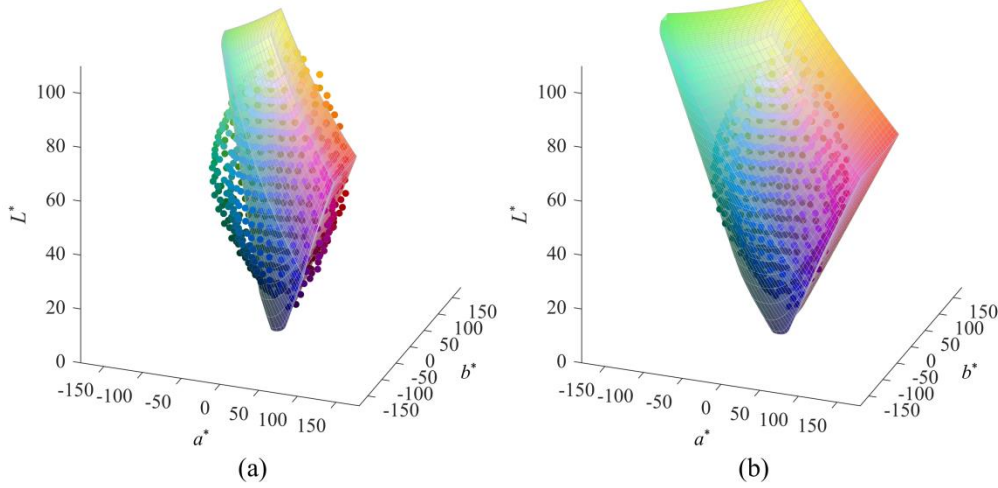
A2.3 Mapping algorithm

Designing a well-tailored gamut mapping algorithm requires careful consideration of the differences between the source and destination gamuts in terms of shape and size. In our gamut mapping algorithm, the out-of-gamut colours (within the region between the BT.2020 and BT.709 gamut boundaries) are mapped onto the BT.709 gamut boundary. The colours within the BT.709 gamut are unchanged, considering a repetitive content exchange between UHDTV and HDTV. It might be reasonable for some textures to become lost if the chroma of the out-of-gamut colours is clipped onto the BT.709 gamut surface. However, most textures consist of lightness variations rather than chroma and hue variations, and texture loss is prevented as long as the lightness variations are retained. On the other hand, colour conversion using a linear matrix (i.e. clipping in the E_R, E_G, E_B channels within the extremes of the coding range after a 3×3 linear-light matrix operation) often creates some flat portions with extreme values in the E_R, E_G, E_B channels, resulting in a loss of texture. In addition to a texture loss, using a popular gamut mapping algorithm to clip the gamut by minimizing the colour differences between the out-of-gamut colours and the mapped colours results in colour discontinuity artefacts [2].

In our algorithm, the CIELAB colour space is utilized for calculating the colour attributes with video levels ranging from 0 to 109 IRE for the E_R, E_G, E_B channels. Figure A2-2 shows the Recommendation ITU-R BT.709 and Recommendation ITU-R BT.2020 gamuts in the CIELAB colour space. The CIELAB formula is used extendedly for overwhite levels up to the maximum lightness value of 106.9. To prevent an excessive chroma reduction in gamut mapping, the lightness of the out-of-gamut colours is changed. The CIELAB metric hues of the out-of-gamut colours, with the exception of yellow highlights and cyan, are designed to be retained. The CIELAB metric hue for yellow highlights is intentionally changed, thereby preventing excessive chroma loss when mapped toward the BT.709 gamut boundary. The CIELAB metric hue for cyan is modified to predict the perceived cyan hue more correctly. The following subsections provide mathematical expressions for the lightness and hue mapping of an out-of-gamut colour ($L_{out}^*, a_{out}^*, b_{out}^*$), with a chroma of $C_{out}^* (= \{(a_{out}^*)^2 + (b_{out}^*)^2\}^{1/2})$ and a hue angle of $h_{out} (= \arctan(b_{out}^*/a_{out}^*))$, to a colour on the BT.709 gamut boundary ($L_{map}^*, a_{map}^*, b_{map}^*$), with a chroma of $C_{map}^* (= \{(a_{map}^*)^2 + (b_{map}^*)^2\}^{1/2})$ and a hue angle of $h_{map} (= \arctan(b_{map}^*/a_{map}^*))$.

FIGURE A2-2

BT.709 gamut (a) and BT.2020 gamut (b) with Pointer colours (under D65) in the CIELAB colour space



A2.4 Lightness mapping

In each constant hue section, the out-of-gamut colours are mapped onto the BT.709 gamut boundary along the lines toward the focal point on the lightness axis, L_{focal}^* , or along the radial lines emanating from the focal point on the chroma axis, C_{focal}^* . Figure A2-3 shows diagrams of BT.709 and BT.2020 gamut boundaries in the constant hue planes along with the focal points and mapping paths. To determine the focal points on the lightness and chroma axes, it was first estimated the BT.2020 and BT.709 cusps (the colours at a given hue that have the largest chroma values for each gamut boundary) in each hue section, and found the intersections of the line connecting the cusps with the lightness axis, L_{cusp}^* , as indicated by the dotted line in Fig. A2-4. The focal points on the chroma axis, C_{focal}^* , are determined as the absolute chroma values of the intersection of the line with the chroma axis. Then defined the focal point on the lightness axis, L_{focal}^* , for each hue within a limited range, using a simple profile to prevent excessive chroma loss and unstable lightness with a change in hue in the gamut mapping. In Figure A2-4, L_{focal}^* is indicated by a solid line. The upper (92.74) and lower (57.47) limits correspond to the values of the dips of L_{cusp}^* at a hue angle of 136° and 306.3° , respectively. In a constant hue plane, the out-of-gamut colours above the L_{focal}^* - C_{focal}^* line (i.e. $L_{out}^* \geq -L_{focal}^* C_{out}^* / C_{focal}^* + L_{focal}^*$) are mapped along the lines toward L_{focal}^* onto the BT.709 gamut boundary as follows:

$$L_{map}^* = \frac{(L_{out}^* - L_{focal}^*) C_{map}^*}{C_{out}^*} + L_{focal}^* \quad (2-1)$$

Whereas those under the line are mapped along the radial lines emanating from C_{focal}^* onto the BT.709 gamut boundary as follows:

$$L_{map}^* = \frac{L_{out}^* (C_{out}^* - C_{map}^*)}{C_{focal}^* - C_{out}^*} + L_{out}^* \quad (2-2)$$

Here, C_{map}^* is determined through this lightness mapping accompanied with the chroma mapping described in the next section.

FIGURE A2-3

BT.709 and BT.2020 gamut boundaries in constant hue planes with focal points and mapping paths

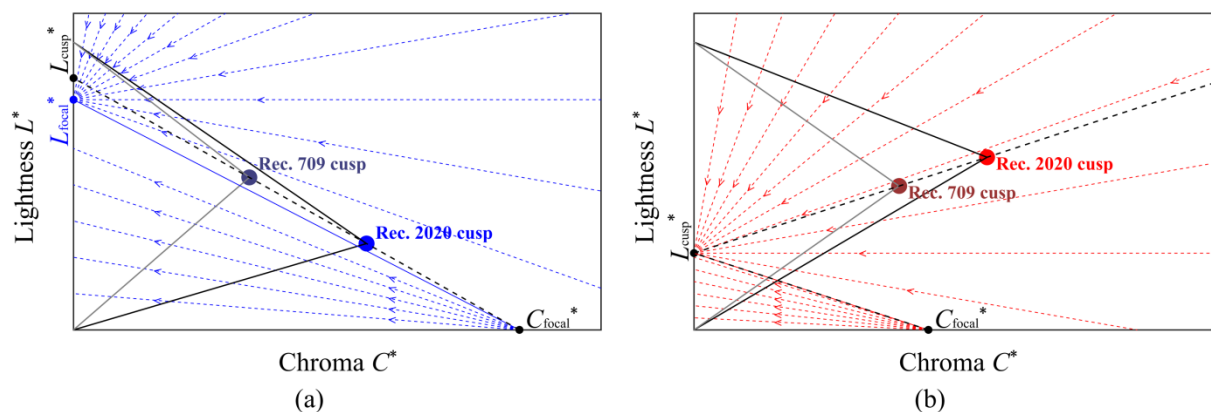
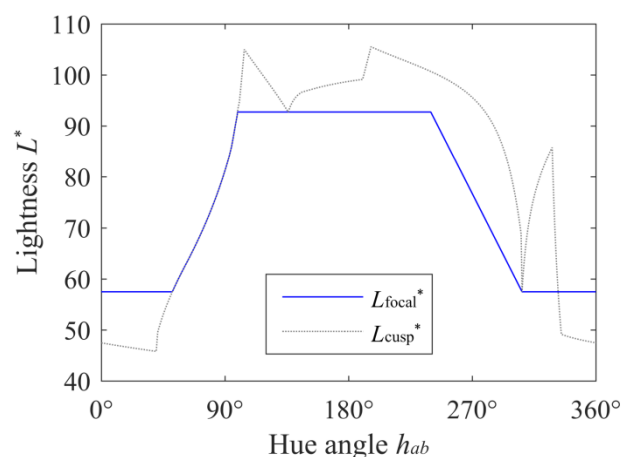
(a) $L_{focal}^* \neq L_{cusp}^*$ and (b) $L_{focal}^* = L_{cusp}^*$ 

FIGURE A2-4

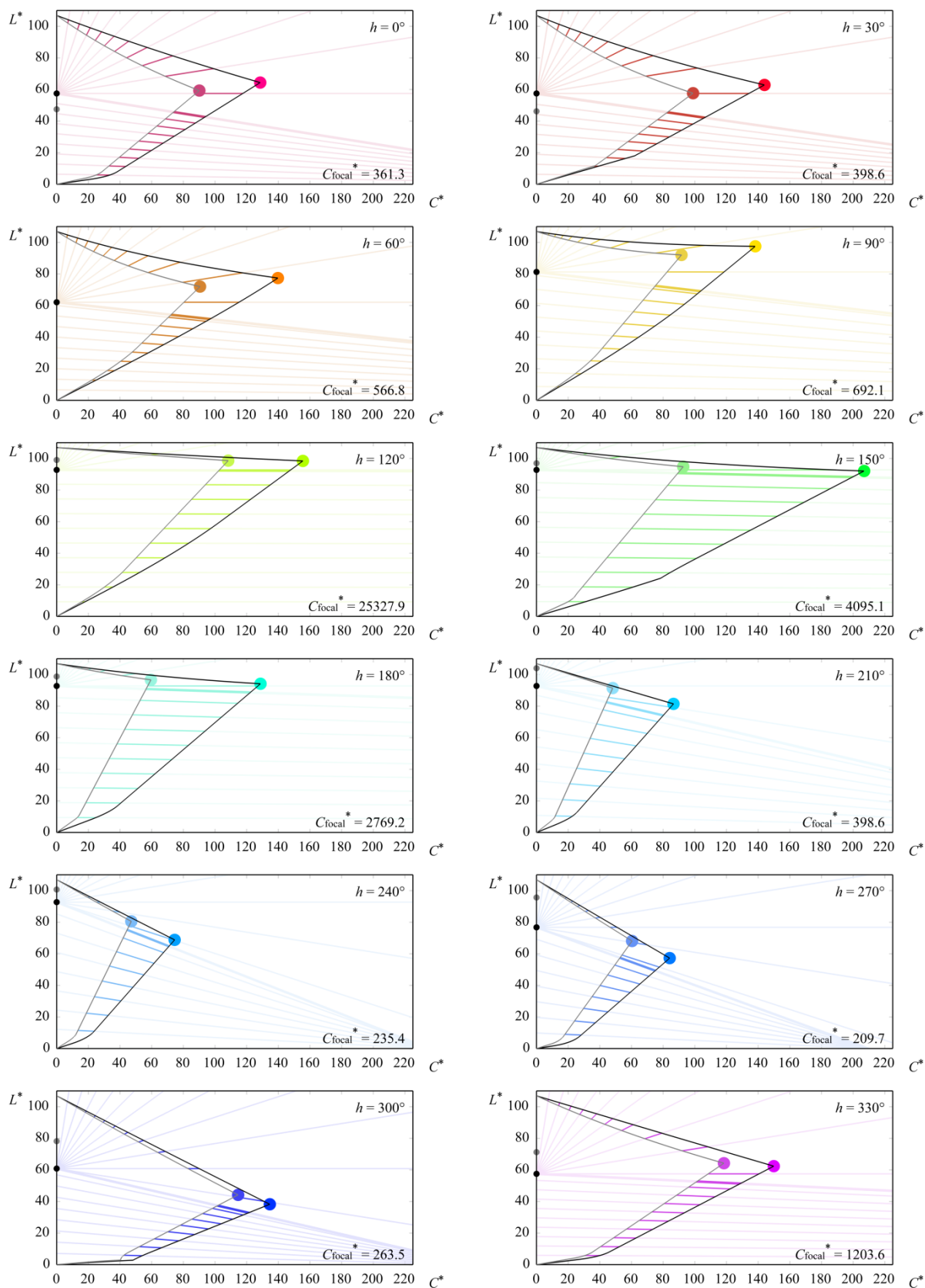
Focal values (L_{focal}^*) on the lightness axis over the hue angle

(The dotted line indicates the lightness values (L_{cusp}^*) of the intersections of the line connecting the BT.2020 and BT.709 cusps with the lightness axis.)

Figure A2-5 shows the boundaries at the constant hue sections ($h_{ab} = 0^\circ, 30^\circ, 60^\circ, 90^\circ, 120^\circ, 150^\circ, 180^\circ, 210^\circ, 240^\circ, 270^\circ, 300^\circ, \text{ and } 330^\circ$) in the CIELAB C^*L^* planes. Excessive chroma reduction can be prevented through this mitigation of the constant lightness condition. For yellow highlights ($0^\circ < h_{ab} < 180^\circ, L^* > 92.74$) and cyan ($180^\circ < h_{ab} < 240^\circ$), whose mapping paths deviate from the radial lines starting from the white point, the lightness values are mapped along each of the lightness mapping paths corresponding to the original hue angles.

FIGURE A2-5

BT.2020 and BT.709 gamut boundaries in constant hue sections ($h_{ab} = 0^\circ, 30^\circ, 60^\circ, 90^\circ, 120^\circ, 150^\circ, 180^\circ, 210^\circ, 240^\circ, 270^\circ, 300^\circ, \text{ and } 330^\circ$) in the CIELAB C^*L^* planes



(The colours outside the BT.709 gamut are mapped along the coloured lines in each constant hue section. The black and gray dots are L_{focal}^* and L_{cusp}^* , respectively.)

A2.5 Hue mapping

In real video contents, the video levels of yellow highlights often reach the extremes of the coding range in the red and green channels. If the colour is mapped to the BT.709 gamut boundary with the CIELAB metric hue remaining unchanged, it causes a blown-out white area with overly desaturated yellow highlights owing to an excessive chroma loss. Figure A2-6 (a) shows the BT.2020 and BT.709 gamut boundaries at a lightness level of 104 with BT.2020 and BT.709 yellow colours having E_R, E_G, E_B IRE levels of (109, 109, 0). If the BT.2020 yellow colour is mapped along the line toward the origin as indicated by the dotted line (i.e. leaving the CIELAB metric hue unchanged), the chroma is excessively reduced. This excessive reduction can be prevented if the mapping paths are slightly changed, as indicated by the yellow loci in Fig. A2-6 (a).

In addition, out-of-gamut cyan consistently appears greenish when compared with a colour on the BT.709 gamut surface having an identical CIELAB metric hue angle. Figure A2-6 (b) shows the BT.2020 and BT.709 gamut boundaries at a lightness level of 95 with BT.2020 and BT.709 cyan colours having E_R, E_G, E_B IRE levels of (0, 109, 109) and constant perceived hues for cyan (see § A2.2). The cyan mapping paths indicated by the cyan loci in Fig. A2-6 (b) roughly predict the constant perceived hue, and the use of the modified mapping paths in the gamut mapping can prevent a greenish appearance of the saturated cyan colours.

Except for the yellow highlights ($0^\circ < h_{\text{out}} < 180^\circ$, $L_{\text{out}}^* > 92.74$) and cyan ($180^\circ < h_{\text{out}} < 240^\circ$), the colour coordinates of a_{map}^* and b_{map}^* of a colour on the BT.709 gamut boundary mapped from an out-of-gamut colour with the colour coordinates of a_{out}^* and b_{out}^* are calculated as follows:

$$(a_{\text{map}}^*, b_{\text{map}}^*) = (ra_{\text{out}}^*, rb_{\text{out}}^*) \quad (2-3)$$

otherwise,

$$(a_{\text{map}}^*, b_{\text{map}}^*) = (a_{\text{out}}^* + m^{-1}(r-1)b_{\text{out}}^*, rb_{\text{out}}^*) \quad (2-4)$$

The parameter value of r is determined such that each out-of-gamut colour is mapped to the BT.709 gamut boundary in this hue mapping accompanied with the lightness mapping described in the previous section.

For a yellow highlight, m in equation (2-4) indicates the slope of the line that connects the BT.2020 yellow colour ($h_{\text{out}} = 98.9^\circ$) and BT.709 yellow colour with the E_R, E_G, E_B IRE levels of (109, 109, 0) on the a^*b^* plane, depending on the hue angle h_{out} of the out-of-gamut colour as follows:

$$m^{-1} = \cot(h_{\text{out}} - 9.137 k \sin(h_{\text{out}})) \quad (2-5)$$

where:

$$k = \begin{cases} (L_{\text{out}}^* - 92.74) / (100.0 - 92.74) & 92.74 < L_{\text{out}}^* \leq 100.0 \\ (106.9 - L_{\text{out}}^*) / (106.9 - 100.0) & 100.0 < L_{\text{out}}^* \end{cases} \quad (2-6)$$

The values of 92.74 and 106.9 correspond to the upper limit of L_{focal}^* and the lightness value of the peak white level, respectively.

For cyan, m in equation (2-4) indicates the slope of the line that connects the BT.2020 cyan colour ($h_{\text{out}} = 190.3^\circ$) and BT.709 cyan colour with the E_R, E_G, E_B IRE levels of (0, 109, 109) on the a^*b^* plane as follows:

$$m^{-1} = \cot(h_{\text{out}} + 10.13 \sin(3h_{\text{out}})) \quad (2-7)$$

The yellow and cyan curves shown in Fig. A2-7 illustrate the loci of the mapping paths based on equations (2-4) through (2-7) in the constant lightness sections ($L^* = 5, 10, 20, 30, 40, 50, 60, 70, 80, 90, 95, 100, 102, 104$, and 106) in the CIELAB a^*b^* planes. The mapping paths for the two colours deviate from the radial lines generated from the white point. The other colours are mapped toward the white point along the radial lines.

FIGURE A2-6

BT.2020 and BT.709 gamut boundaries and mapping loci

- (a) Gamut boundaries at a lightness level of 104 with BT.2020 and BT.709 yellow colours having RGB IRE levels of (109, 109, 0), and
- (b) gamut boundaries at a lightness level of 95 with BT.2020 and BT.709 cyan colours having RGB IRE levels of (0, 109, 109) and constant perceived hues for cyan

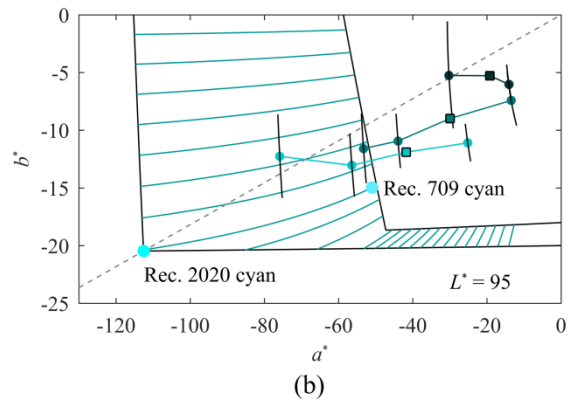
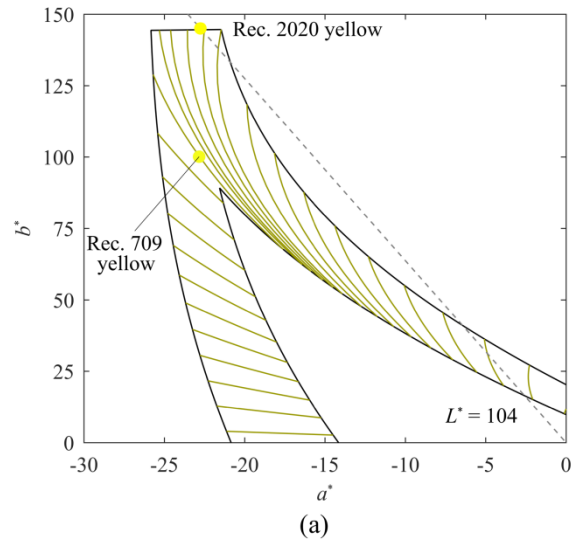
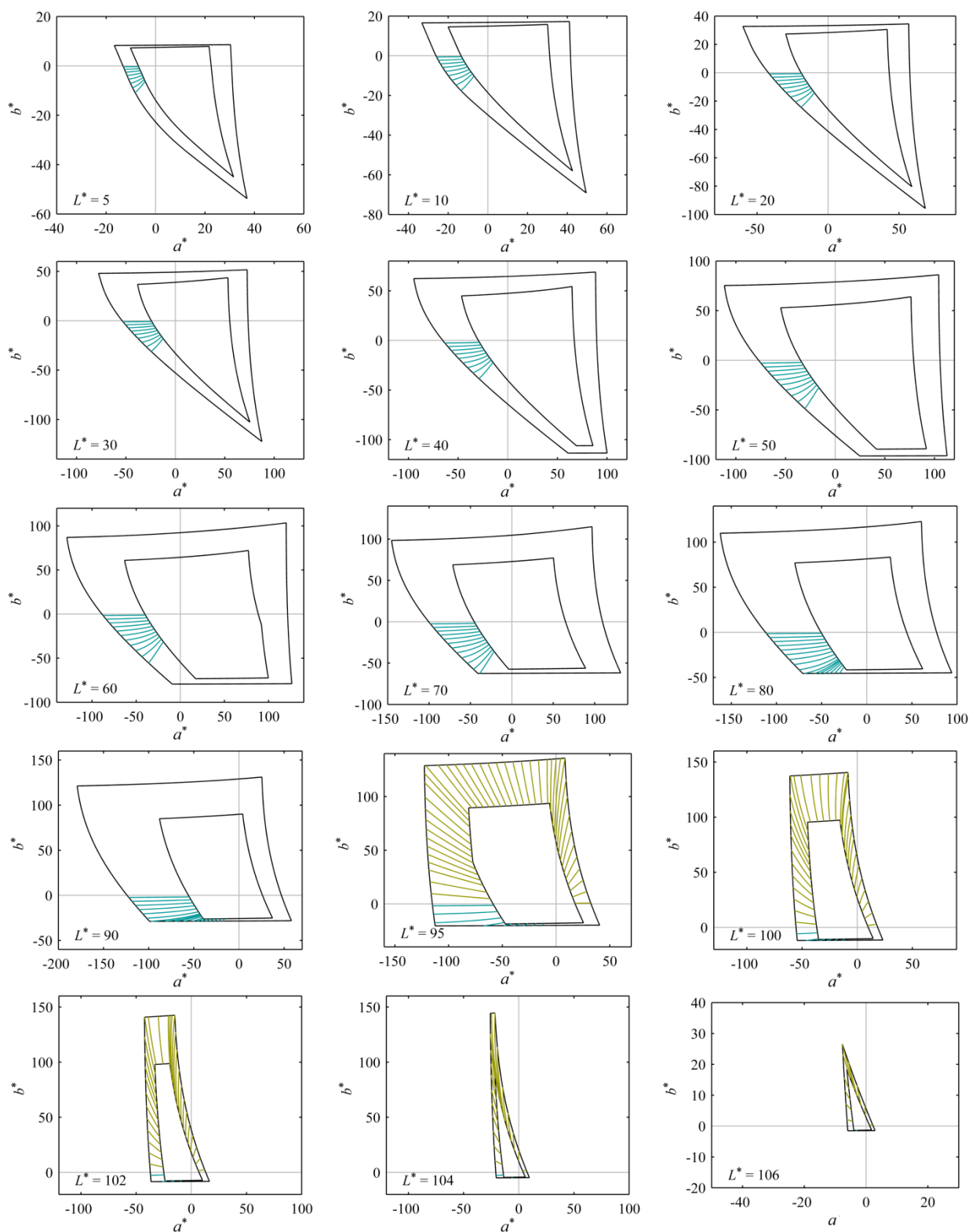


FIGURE A2-7

BT.2020 and BT.709 gamut boundaries in constant lightness sections
 ($L^* = 5, 10, 20, 30, 40, 50, 60, 70, 80, 90, 95, 100, 102, 104, \text{ and } 106$) in the CIELAB a^*b^* planes



(The out-of-gamut yellow highlights ($0^\circ < h_{ab} < 180^\circ$, $L^* > 92.74$) and cyan ($180^\circ < h_{ab} < 240^\circ$) are mapped along the yellow and cyan loci, respectively, and other colours are mapped along the radial lines emanating from the origin.)

A2.6 Image quality

Figure A2-8 shows a wide-gamut image encoded using BT.2020 E_R, E_G, E_B , as well as images converted using the combined gamut mapping algorithm and another algorithm utilizing the method based on linear matrix transformation. Some petals of the red roses are no longer distinct in the E_R, E_G, E_B clipping, whereas those in the combined gamut mapping remain separated. Figure A2-9 shows wide-gamut images encoded using BT.2020 E_R, E_G, E_B , as well as those reproduced based on the combined gamut mapping algorithm and another algorithm utilizing chroma clipping (i.e. while preserving the CIELAB metric hue and lightness of the out-of-gamut colours but reducing the chroma until the gamut boundary is reached). Through the combined method, excessive chroma loss is not observed in the yellow highlights, and the perceived hue of the cyan is improved.

FIGURE A2-8

Comparison of images converted from BT.2020 image



Original



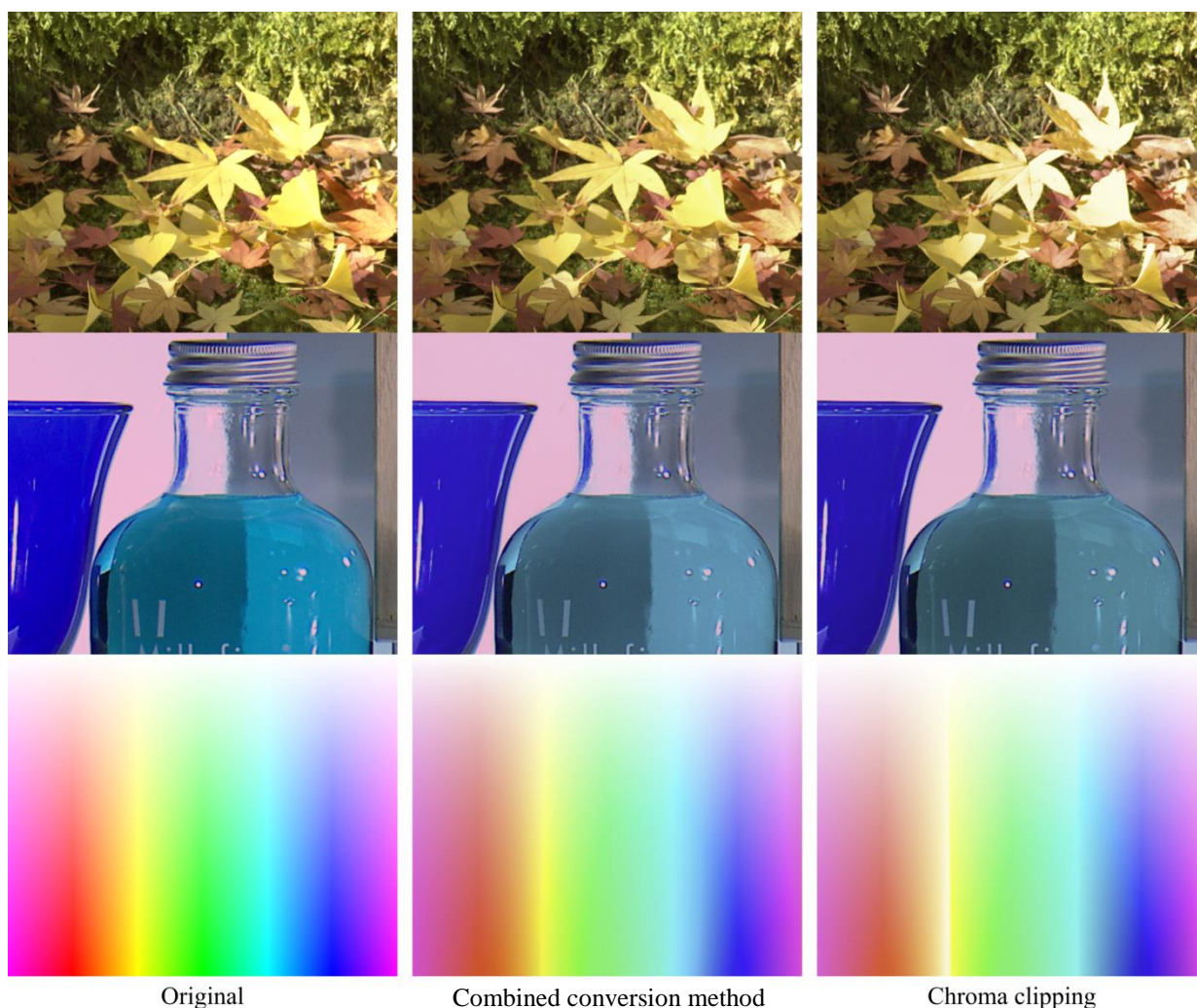
Combined conversion method



Method based on linear matrix transformation

NOTE – The images should be viewed on BT.2020 displays, although artefacts from the RGB clipping (texture loss) can be seen on BT.709/sRGB displays.

FIGURE A2-9
Comparison of converted BT.2020 images



NOTE – The images should be viewed on BT.2020 displays, although artefacts from the chroma clipping (blown-out yellow highlights and greenish cyan) can be seen on BT.709/sRGB displays.

A2.7 Implementation

The combined gamut mapping algorithm was implemented in a real-time gamut converter with a dual-link HD-SDI input/output (1080/60/I, RGB 4:4:4, 10 bits) and a 3D lookup table of $129 \times 129 \times 129$ grid points. The conversion method from BT.2020 to BT.709 using a laser-backlit 4K LCD [11] and an HDTV mastering monitor was presented in 2015 at the NHK STRL Open House [12].

References

- [1] K. Masaoka, Y. Kusakabe, T. Yamashita, Y. Nishida, T. Ikeda, and M. Sugawara, “Algorithm Design for Gamut Mapping from UHDTV to HDTV,” J. Display Technol. (to be published).
- [2] J. Morovic, *Colour Gamut Mapping*, 1st ed. England: Wiley, 2008.
- [3] CIE Technical Report 159:2004, “A Colour Appearance Model for Colour Management Systems: CIECAM02,” International Commission on Illumination, Vienna, 2004.

- [4] J. Fröhlich, A. Schilling, and B. Eberhardt, “Gamut mapping for digital cinema,” *SMPTE Mot. Imag J.*, vol. 123, no. 8, pp. 41–48, 2014.
- [5] J. Morovic, V. Cheung, and P. Morovic, “Why we don’t know how many colours there are,” in *Proc. 6th European Conference on Colour in Graphics, Imaging, and Vision*, Amsterdam, Netherlands, 2012, pp. 49–53.
- [6] F. Ebner and M. D. Fairchild, “Development and testing of a colour space (IPT) with improved hue uniformity,” in *Proc. IS&T/SID 6th Colour Imaging Conference*, Scottsdale, AZ, 1998, pp. 8–13.
- [7] K. Masaoka, T. Yamashita, Y. Nishida, and M. Sugawara, “Heuristic approach to selecting a colour appearance model for hue-preserved wide-colour gamut mapping,” *J. Soc. Info. Display*, vol. 23, no. 3, pp. 113–118, 2015.
- [8] Y. Iwasaki, K. Masaoka, Y. Kusakabe, and Y. Nishida, “Subjective evaluation of constant perceived hue in the UHDTV wide-gamut,” *IEICE Technical Report*, vol. 114, no. 171, pp. 1–5, 2014 (in Japanese).
- [9] N. Moroney, “Assessing hue constancy using gradients,” in *Proc. SPIE*, 2000, vol. 3963, pp. 294–300.
- [10] K. Masaoka, Y. Nishida, M. Sugawara, and E. Nakasu, “Design of primaries for a wide-gamut television colourimetry,” *IEEE Trans. Broadcast*, vol. 56, no. 4, pp. 452–457, 2010.
- [11] E. Niikura, N. Okimoto, S. Maeda, H. Yasui, A. Heishi, S. Yamanaka, T. Sasagawa, Y. Nishida, and Y. Kusakabe, “Development of RGB laser backlit liquid crystal display,” in *Proc. 22nd International Display Workshops*, Otsu, Japan, 2015.
- [12] NHK STRL OPEN HOUSE (2015) [Online].
Available: http://www.nhk.or.jp/strl/open2015/en/tenji_10.html.

Annex 3

A simple, low-complexity and parametric conversion method for lower-end production is presented. It is a modular method according to Fig. A1-1.

The simple conversion method operates in a simplified CIELAB colour space. These coordinates are calculated from CIEXYZ colour coordinates according to:

$$\begin{aligned}
 L_S &= 100 \cdot \left(\frac{Y}{Y_n} \right)^{1/3} \\
 a_S &= 500 \cdot \left(\left(\frac{X}{X_n} \right)^{1/3} - \left(\frac{Y}{Y_n} \right)^{1/3} \right) \\
 b_S &= 200 \cdot \left(\left(\frac{Y}{Y_n} \right)^{1/3} - \left(\frac{Z}{Z_n} \right)^{1/3} \right)
 \end{aligned}$$

This colour space generates colour gamuts having linearized shape in the lower part of the colour gamut (characterized by straight lines passing through the colour space origin), i.e. for colours that can be represented by one or two primary colours. However, other colour spaces such as CIELAB or IPT can be used.

Hue is defined as the polar angle of the vector $\begin{pmatrix} a_S \\ b_S \end{pmatrix}$. Hue is an aspect of colour that should generally be preserved during conversion; however, if wanted for a specific application, a hue mapping method according to § A1.1 or § A2.5 may be applied.

Lightness is an aspect of colour that should be modified very carefully during conversion in order to avoid unwanted change of brightness and contrast. However, a lightness mapping method according to § A1.2 or § A2.4 may be applied. For example, the lightness mapping described in § A1.2 is controlled by the cusp lines of the colour gamuts. These cusp lines can be approximated by piecewise linear functions of hue. The lightness mapping operates then within a constant-hue leaf according to:

$$L'_S = L_S + (L_{Cusp}^{709} - L_{Cusp}^{2020}) \cdot \frac{C_S}{C_{Cusp}^{2020}}$$

where L_{Cusp}^{709} is the lightness of the cusp of the BT.709 gamut in the hue leaf of the source colour, L_{Cusp}^{2020} and C_{Cusp}^{2020} are the lightness and the chroma, respectively, of the cusp of the BT.2020 colour gamut, and L'_S is the mapped lightness of the source colour. This well-known cusp-to-cusp principle maps the cusp colour of the source colour gamut onto a colour having the lightness of the cusp colour of the target colour gamut. This lightness mapping simplifies the geometry of the chroma mapping significantly. However, lightness mapping is optional and the following chroma mapping is described as if there were no lightness mapping.

Chroma is defined as the Euclidean norm of the vector $\begin{pmatrix} a_s \\ b_s \end{pmatrix}$. For chroma mapping, a simple, two-step approach is proposed. Chroma mapping is first defined for those source colours having the same hue as one of the primary and secondary colours of the source colour gamut (BT.2020) or the target colour gamut (BT.709), see Fig. A3-1. These hues are called key hues. For example colours having same hue as the BT.2020 green primary are mapped according to:

$$C_T = C_{T,max} \cdot f_{G2020} \left(\frac{C_S}{C_{S,max}} \right)$$

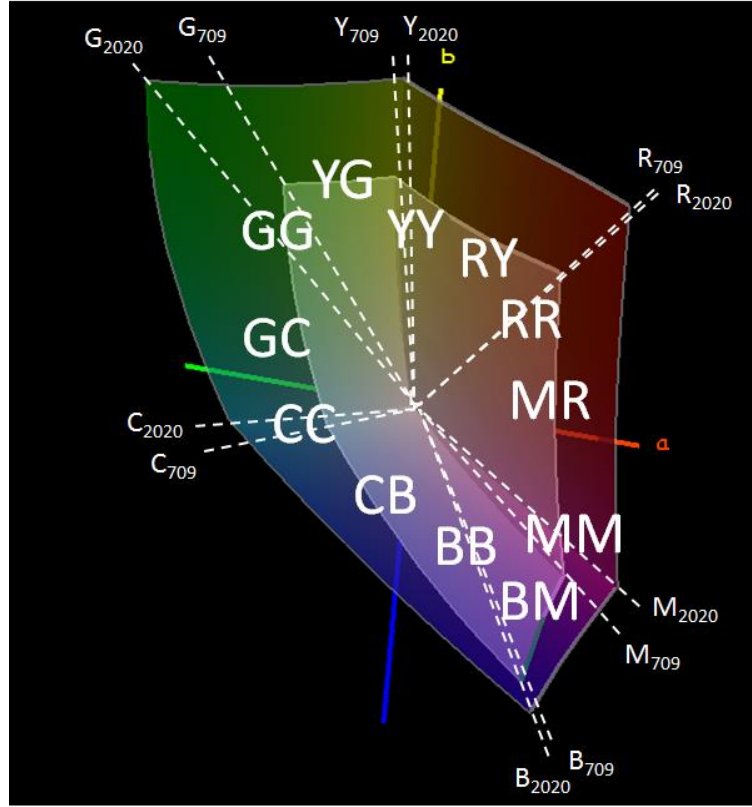
where $G2020$ indicates the key hue, here the hue of the BT.2020 green primary. $C_{S,max}$ and $C_{T,max}$ are the maximum possible chroma values at same hue and lightness as the source colour in the source colour gamut (BT.2020) and in the target colour gamut (BT.709), respectively. For example, for colours having the same lightness as the BT.2020 green primary, $C_{S,max}$ is the chroma of the BT.2020 green primary. The mapping function:

$$f_{G2020} \left(\frac{C_S}{C_{S,max}} \right) = \sum_k u_{G2020,k} \cdot \left(\frac{C_S}{C_{S,max}} \right)^k$$

is a polynomial with parameters $u_{G2020,k}$. The mapping function and its parameters $u_{G2020,k}$, here for the BT.2020 green primary, have to be defined for each of the 12-key hues according to artistic mapping preferences or by fitting to a given conversion method, for example one of the methods 1 and 2 described in Annex 1 and Annex 2. More key hues can be used if specific colours should be mapped in a specific way, for example skin tones.

FIGURE A3-1

12 primary/secondary colours red (R), yellow (Y), green (G), cyan (C), blue (B), magenta (M) of BT.2020 and BT.709, and 12 hue sections RR, RY, YY, YG, GG, GC, CC, CB, BB, BM, MM, MR defined by these 12 colours



Using the mapping functions of the 12 key hues, the mapping of all source colours is defined in each of the 12 angular hue sections shown in Fig. A3-1. For example, colours lying in the hue section GC between the BT.2020 green primary colour G_{2020} and the BT.2020 cyan secondary colour C_{2020} are mapped according to:

$$C_T = C_{T,max} \cdot f_{GC} \left(h, \frac{c_s}{c_{s,max}} \right)$$

Thanks to the described cusp-to-cusp lightness mapping and thanks to the use of the simplified CIELAB colour space, $C_{s,max}$ and $C_{T,max}$ can be approximated for each hue section using piecewise linear functions of hue and lightness. In fact, in each hue leaf, the ratio:

$$\frac{C_{s,max}}{C_{T,max}} = \frac{C_{Cusp}^{2020}}{C_{Cusp}^{709}}$$

is constant for colours with lightness below the cusp and approximately constant for the other colours. The mapping function f_{GC} is also defined by a polynomial:

$$f_{GC}(h, w) = \sum_k u_{GC,k}(h) \cdot w^k$$

with the same structure as $f_{G_{2020}}$ but its coefficients are interpolated over the hue section GC according to:

$$u_{GC,k}(h) = (h - h_{G_{2020}}) \cdot \left(\frac{u_{C_{2020},k} - u_{G_{2020},k}}{h_{C_{2020}} - h_{G_{2020}}} + (h - h_{C_{2020}}) \cdot \sum_j v_{GC,j,k} \cdot h^j \right) + u_{G_{2020},k}$$

where h is the hue of the source colour. The parameters $v_{GC,j,k}$ that characterize this mapping function have to be defined for each of the 12 or more hue sections according to artistic mapping preferences or by fitting to a given conversion method, for example one of methods 1 and 2 described in Annex 1 and Annex 2.

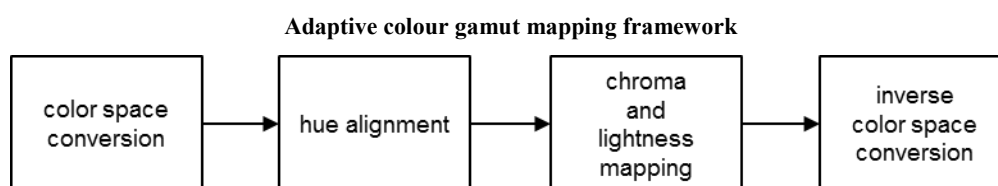
Annex 4

In the following sections, the design process of the adaptive gamut mapping framework is described.

A4.1 Adaptive gamut mapping framework

The adaptive colour gamut mapping framework aims to preserve perceptual colourfulness of the original image. To reduce loss of colour saturation and loss of colour difference caused by large to small colour gamut mapping process, the core region where the colour change is minimized is proposed to use on a constant-hue-angle-plane. By using the core region, both in- and out-of-target-colour-gamut colour components in BT.2020 container could preserve colourfulness with distinctive colours near the colour gamut boundary. The mapping process on a constant-hue-angle-plane is designed to prevent chroma inversion artefact especially for max chroma of each hue plane. The detailed process of the adaptive colour gamut mapping framework is described as follows:

FIGURE A4-1



A4.1.1 Colour space conversion

In colour gamut mapping algorithms, selection of colour space is an important step since the colour gamut mapping resultant depends on the characteristics of colour space as well as the mapping methodology. As an example, if one uses YCbCr colour space for a colour management process, a modification in one channel could affect to the others unintendedly due to the inter-channel dependency.

Among the colour spaces, CIELAB colour space is well studied and widely used in colour gamut mapping algorithms. As the colour space is designed to separate lightness and colourfulness, which are described by L axis itself and a chroma plane made by a and b axis, respectively, most of the colour gamut mapping algorithms performs channel independent process by adopting CIELAB colour space. Similar to those approaches, the adaptive colour gamut mapping framework also uses CIELAB colour space to take an advantage from the separate process on each component such as hue, lightness, and chroma.

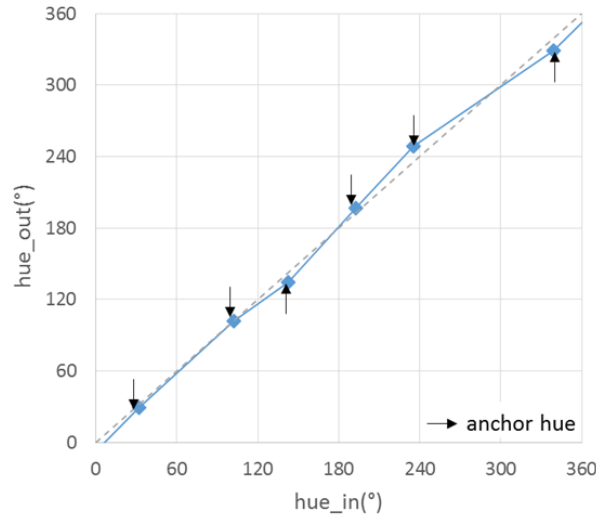
A4.1.2 Hue alignment

To minimize the hue distortion in the mapping process, the adaptive colour gamut mapping is performed on a constant-hue-angle-plane which preserves hue angle during the lightness and chroma mapping. One prominent issue when applying this approach to the mapping between BT.2020 and BT.709 is the hue angle mismatch between corresponding colours in each colour gamut. For example, when the misalignment is not considered, the blue primary colour in the source gamut is not mapped to the corresponding blue primary colour so that the order of the chroma values near the blue primary colour will be reversed.

To prevent distortion caused by the primary mismatch between two colour gamuts, hue alignment is performed before the lightness and chroma mapping. In this step, all hue angles of source colour gamut are aligned to the correspondences in target colour gamut by minimizing the hue angle gap between colours matched in source and target colour gamut. In the adaptive gamut mapping

framework, the primary and secondary colours are selected as a representative colour components and hue angle gap between those colours are minimized as shown in Fig. A4-2.

FIGURE A4-2
Hue alignment from ITU-R BT.2020 to ITU-R BT.709



A4.1.3 Chrominance mapping with lightness constraint

In the adaptive colour gamut mapping framework, the lightness and chroma on each constant-hue-angle-plane are managed to have perceptually similar colourfulness as well as similar colour difference between adjacent components. To achieve both goals, the adaptive gamut mapping framework adopts core region where each component keeps the colourfulness of the source colour. The out of core region colours are mapped to be placed within the target gamut boundary while keep the relative difference between neighbouring colours. To avoid chroma inversion artefact, the core region and the mapping trajectory are carefully designed as follows.

A4.1.3.1 Core region

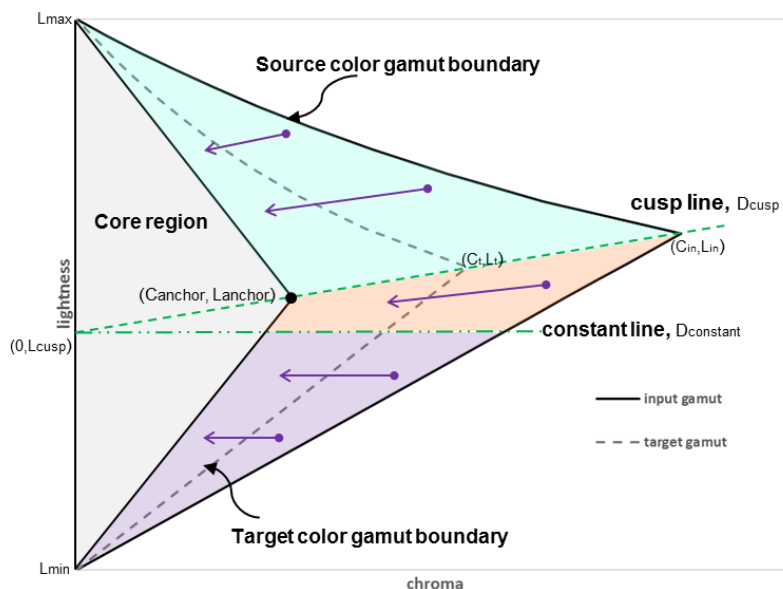
Colour gamut mapping from a large colour volume to a smaller one is an underdetermined problem that does not have a unique solution. One of the well-known approaches is clipping which leaves the colour in the intersecting area of two colour gamut and then maps the out-of-gamut colours onto the target gamut boundary [1]. With this approach, the colour distribution of in-target-gamut is unchanged by sacrificing colour contrast between colour components presents in between source and target colour boundaries. As another extreme approach, all source colours could be mapped into the target colour volume and preserves relative difference between colour components both in- and out-of-target-gamut. However, it produces less colourful result since all chroma components are moved toward de-saturated direction.

As an alternative approach which considers pros and cons of two extreme cases, the adaptive gamut mapping framework adopts lightness and chroma adaptive mapping by using core region. The main concept of the adaptive gamut mapping framework is to preserve colours in core region while preserving the relative colour difference in the other region. In the adaptive gamut mapping framework, the core region is defined as a closed area in the target colour gamut boundary on a constant-hue-angle-plane.

As a colour component in the core region maintains the original lightness as well as the chroma values, the performance and the percentage of preserving original colour depends on the design of the core region. The boundary shape of the core region is designed to resemble that of the target

colour gamut. In order to consider all lightness level in the core region, the full lightness range of target gamut is covered for achromatic colour. The maximum chroma point of the core region is designed to be on the cusp to cusp line which is a line made by source and target maximum chroma points on a constant-hue-angle-plane. The core region takes the main role to preserve the intended colourfulness. The colourfulness of the original image is highly preserved when the gap between region boundary and the target gamut boundary decreases.

FIGURE A4-3
Adaptive chroma and lightness mapping on a constant-hue-angle-plane



A4.1.3.2 Chroma and lightness mapping

When a colour component to be mapped is determined to be in the out of the core region, the component is mapped into the area between core region boundary and target gamut boundary. In the mapping process performed on the constant-hue-angle-plane basis, chroma and lightness is managed to preserve the colour difference between colour components as well as to prevent chroma inversion artefact.

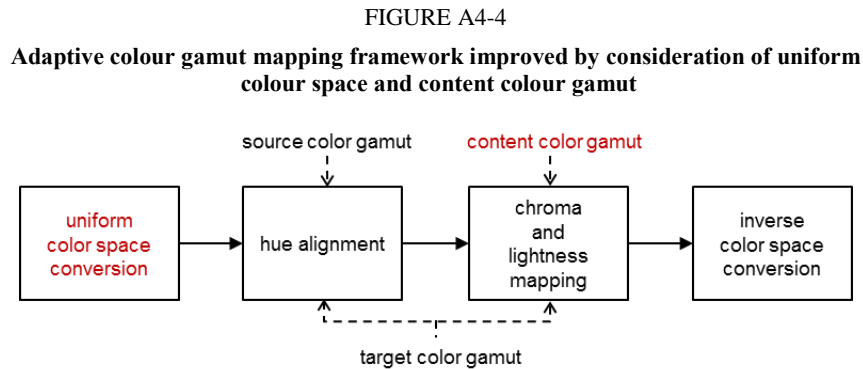
The chroma inversion artefact considered in the adaptive gamut mapping framework occurs near the maximum chroma of source colour gamut. When the maximum chroma of a source colour gamut is not correctly mapped to corresponding maximum target chroma, the resultant image suffers from reversed chroma order especially for the saturated colours. In the adaptive gamut mapping framework, cusp to cusp mapping is adopted to prevent the degradation where cusp means the maximum chroma point of a colour gamut on a constant-hue-angle-plane. As the maximum chroma of the core region also designed to be on the cusp line, the colour points on the cusp line are mapped along the cusp line.

To consider the colour contrast between colour points to be mapped, the mapping trajectory is carefully designed while the mapping direction is changed according to the following three different mapping regions. When a colour point is in the closed region composed by cusp line, source colour gamut boundary and core region boundary where the signs of each slope of the boundary are not equal to the sign of the cusp line slope, the colour component in this region is mapped according to the line parallel to the cusp line. When a point is not included in the mapping region described above, the mapping is directed to the intersection of the cusp line with the lightness axis while the slope of the mapping line has the same sign with that of the cusp line. In the other mapping region, only the chroma component

is changed to be mapped on the constant lightness line. In Figure A4-3, the region adaptive mapping method is described where the three regions are shown in green, orange and purple, respectively.

A4.2 Additional considerations for improved gamut mapping

In this section, factors which improve the performance of a gamut mapping algorithm are discussed. The first one is colour space where the gamut mapping is performed on and directly impact on the design of the gamut mapping algorithm. The second one is content colour gamut boundary where the information could help to reduce the distortion due to the large gap between source and target colour gamut. As an example of adopting those considerations, the adaptive gamut mapping framework described in Fig. A4-1 is modified to Fig. A4-4. In the following, the effect of the advanced colour space and additional colour gamut boundary information is briefly discussed.



A4.2.1 Uniform colour space based on CIECAM02

As discussed in § A4.1.1, the performance of the colour gamut mapping algorithms is generally relying on the characteristics of the colour space used. Although CIELAB effectively separates the colour components, dependency remained in some colour hue produces colour distortion in the resultant of colour gamut algorithms [2]. As an example, it is well known that unintended hue shift is shown on blue colours when colour gamut mapping is performed based on CIELAB colour space. To avoid the problem inherent in the colour space, a colour gamut mapping algorithm can be performed on a colour space based on an advanced colour appearance model, such as CIECAM02 [3] which shows increased inter-channel decorrelation as well as the improved uniformity. As shown in Fig. A4-5, uniform colour space based on CIECAM02 presents high performance on preserving hue component when chroma is changed only. On the other hand, CIELAB colour space shows hue distortion with purple colours when the chroma value is decreased.

In Fig. A4-6, the colour gamut boundaries of BT.2020 and BT.709 colour gamut are described on chroma-hue plane of CIELAB colour space and uniform colour space based on CIECAM02. While the boundary on CIELAB colour space has curved boundary shape, the shape on the advanced colour space shows linearized boundary. This linear boundary helps to adopt advanced colour space with simplified but powerful process and results in improved colour gamut mapping performance.

FIGURE A4-5

Colour space comparison for blue hue patches (chroma changes with constant lightness)

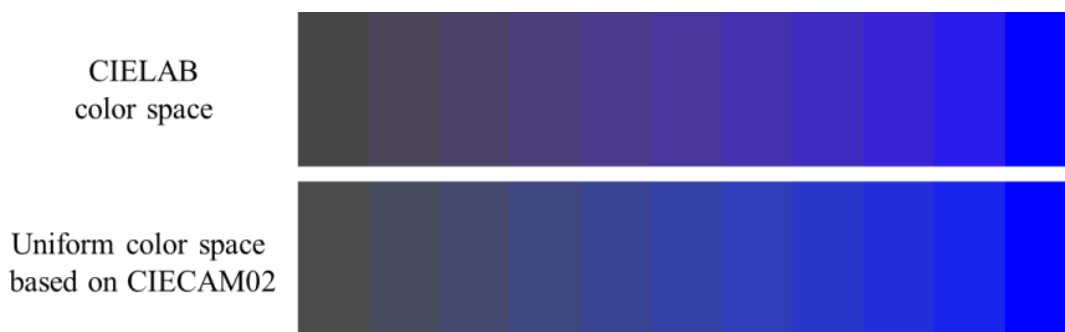
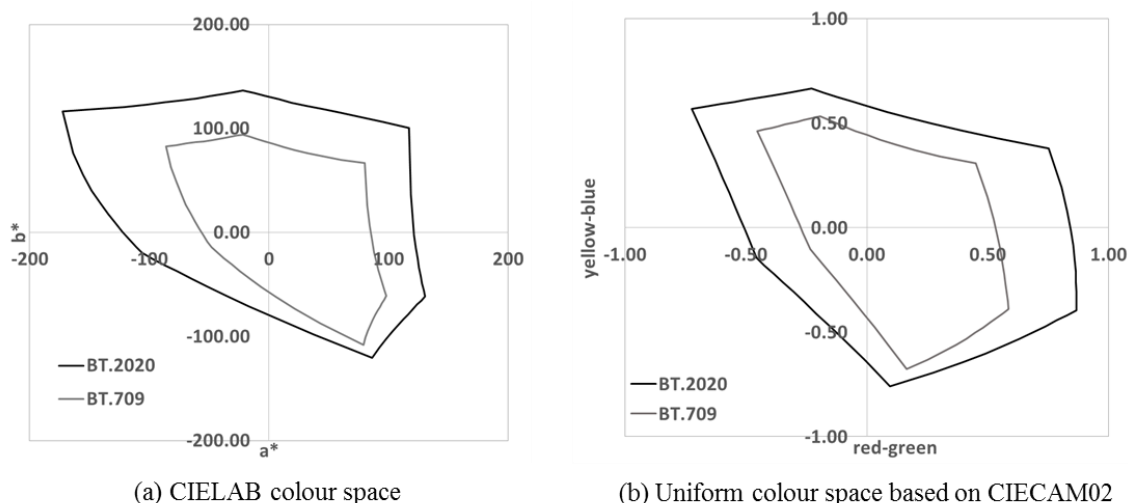


FIGURE A4-6

Colour gamut boundaries on (a) CIELAB colour space, and (b) uniform colour space based on CIECAM02



(a) CIELAB colour space

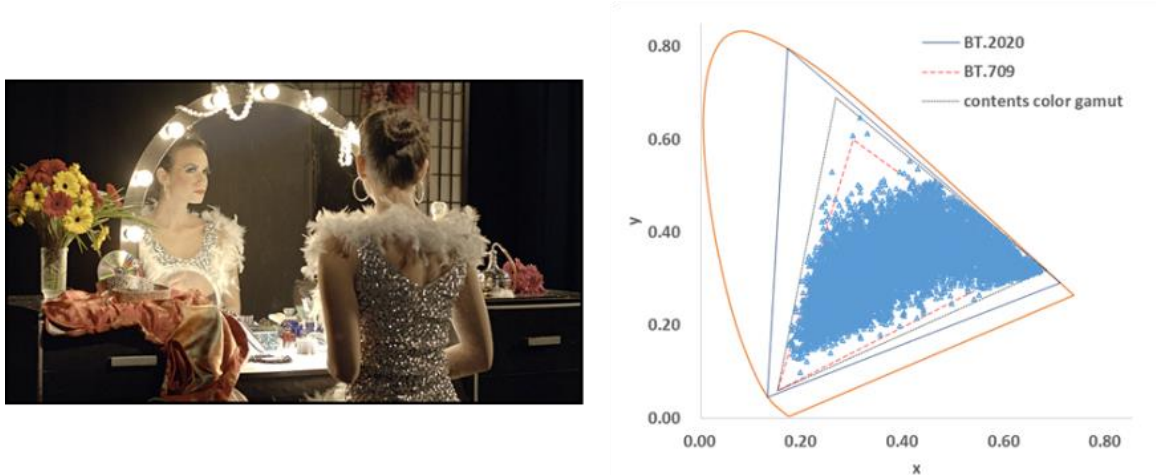
(b) Uniform colour space based on CIECAM02

A4.2.2 Content colour gamut

One of the problems that are not considered in the adaptive gamut mapping framework is the gap between source and target gamut boundaries. In mapping from BT.2020 to BT.709, the gap area between two colour gamuts is so huge that the loss of colourfulness and colour contrast is inherently large. Based on the intention to reduce the gap between two gamuts, gamut boundary which is closer to target gamut could be used as an alternative to the source gamut boundary in colour gamut mapping algorithms. One of the appropriate and reasonable consideration for this problem is a content colour gamut which is defined as an actual distribution of colours in a content or a scene. In Figure A4-7, an example of content colour distribution is depicted with blue dots in CIE1931 xy plane. As shown in the Figure, not all of the area of BT.2020 colour gamut is occupied by the content especially for the saturated colour region near the gamut boundary. Therefore, the content colour gamut could be drawn in the area between BT.709 and BT.2020. When the content colour gamut is used in gamut mapping, the resultant is anticipated to be improved with reduced colour distortion and increased colour contrast due to the reduced gap between source and target gamuts.

FIGURE A4-7

An example of colour distribution of a content in BT.2020 container colour gamut and corresponding content colour gamut



A4.3 Experimental results

In this section, the experimental results of adaptive gamut mapping framework in performing BT.2020 to BT.709 colour gamut mapping are described. At first, the performance of the adaptive gamut mapping framework is examined with description of the effect of the core region. Moreover, the effect of the additional factors, uniform colour space and the content colour gamut, are described respectively. The detailed description of the wide colour gamut test images used in the following experiments is given in [4]. Note that the results are represented in BT.2020 container for all images shown in the following Figures. Thus the display which supports BT.2020 colour space is recommended to be used when viewing the results in order to see the exact colours.

A4.3.1 Experimental result of adaptive gamut mapping framework

As discussed in § A4.1.3.2, the performance of adaptive gamut mapping framework is changed based on core region design. The core region determines the level of preserving colourfulness and details in the saturated colours. To show the effect of core region size, adaptive gamut mapping is performed on simulated image patches with same hue value. In the original image of Fig. A4-8, vertical edges are shown on every boundary between patches due to the chroma difference. When clipping is used with the core region size that is same with the target gamut, the vertical edge between every second and third patches is disappeared due to the same chroma and lightness after the clipping operation. On the other hand, adaptive gamut mapping framework (core region size with 50% of the target gamut area) preserves the edges since the relative chroma difference between patches is preserved.

In Fig. A4-9, the output images of adaptive colour gamut mapping framework are compared for wide colour gamut test images. The first row shows the effect of the core region size where the more colourfulness is preserved when using wider core region. In the second row, the preservation of details according to the core region size is compared. As described in the enlarged images with red solid and dotted line boxes, the colour contrast in the source image is reduced when the saturated yellow colours are mapped onto the target colour gamut boundary by using core region size of 100% of target gamut area. When using smaller core region size with 50% of target gamut area, the colour difference and the details are preserved.

For more detailed comparison in the perspective of preserving colour contrast, the lightness, chroma, and hue values of the selected points from an output image set are calculated. As described in Fig. A4-10, the four colour patches are selected where pair of them are similar in hue and lightness while they are different in the chroma values in the source image. When the core region is set to 100% of the target gamut area, the first and the fourth patch is changed close to the second and the third

patches, respectively, since the adaptive colour gamut mapping method performs as a clipping operation. As can be seen in the enlarged images, the colours of those patches became similar although the original colours are visually distinctive. When the core region size is adjusted to 50%, which preserves relative difference between colour components, the difference between the pairs of patches in pair is relatively preserved with different chroma values while preserving lightness and hue.

FIGURE A4-8

Effect of core region in adaptive colour gamut mapping framework

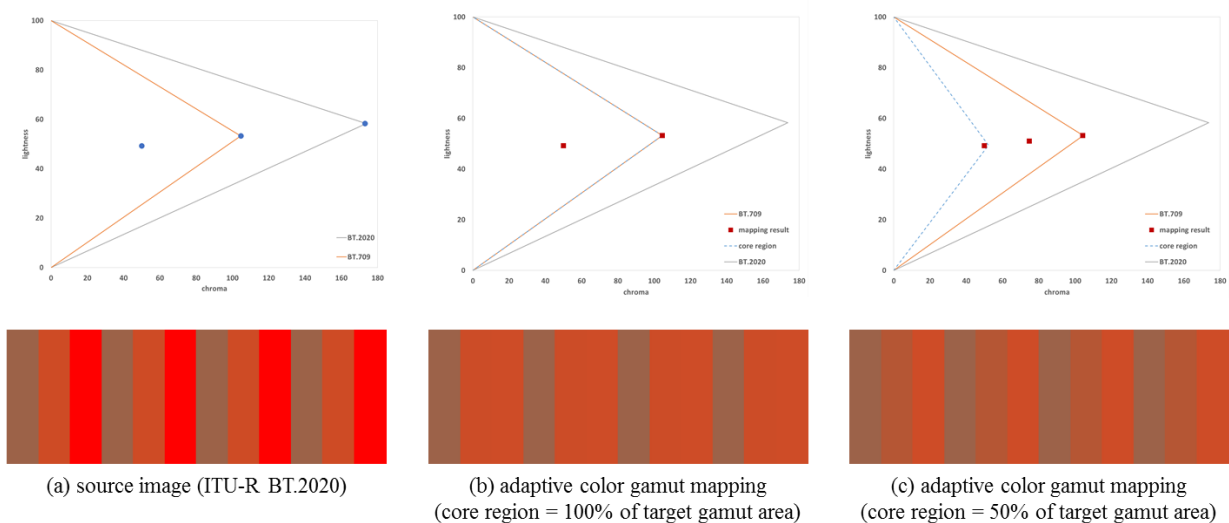


FIGURE A4-9

Results of adaptive colour gamut mapping with different core region size

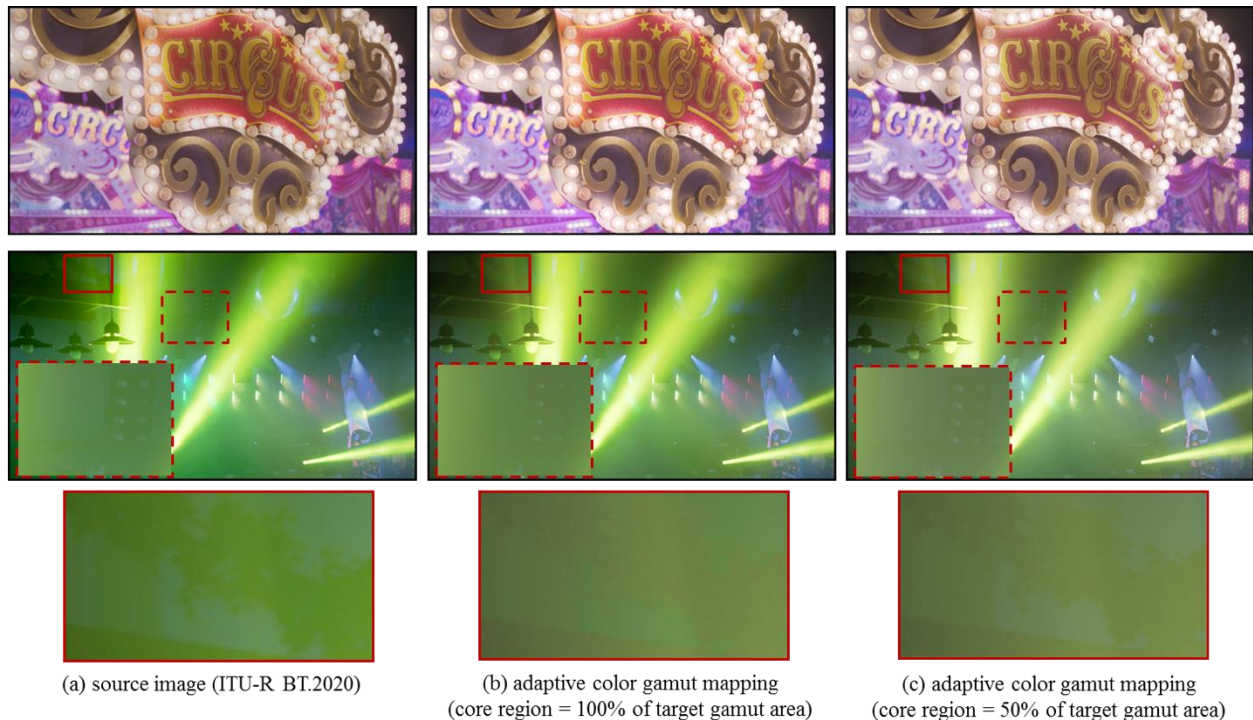
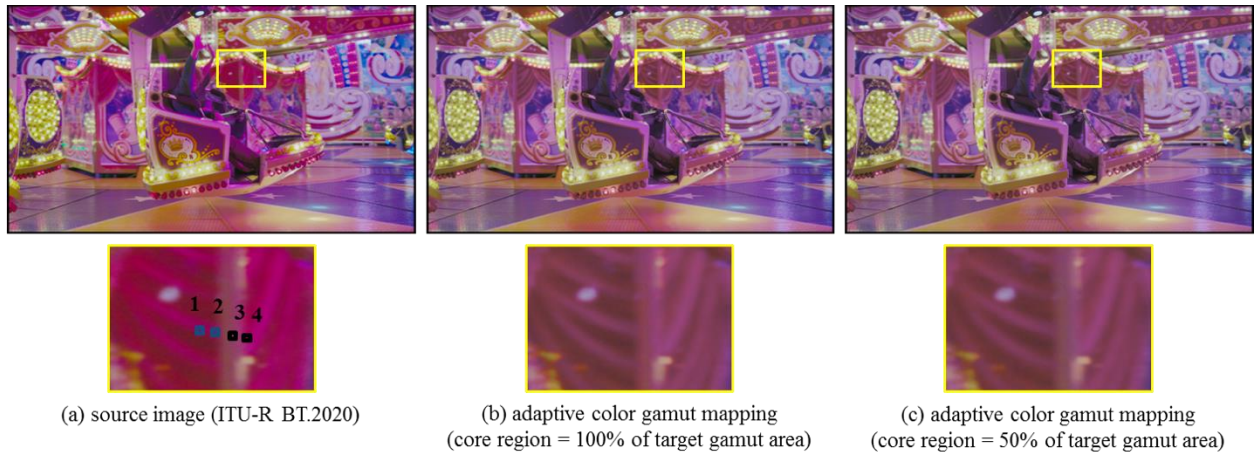








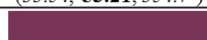
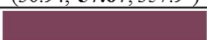
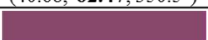
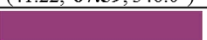


FIGURE A4-10

Comparison of adaptive gamut mapping on colour contrast preservation



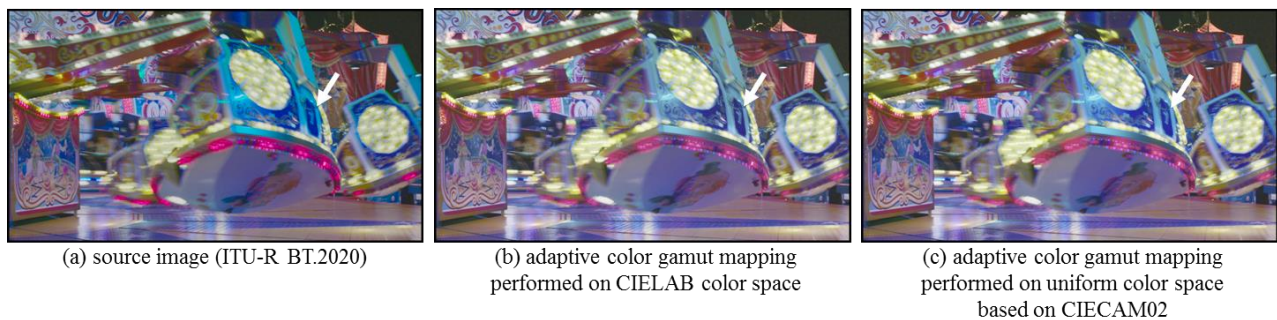
(L,C,h)	patch 1	patch 2	patch 3	patch 4
Source				
	(33.70, 79.54, 359°)	(36.82, 59.40, 2.1°)	(40.68, 62.69, 355.2°)	(41.24, 93.36, 351.0°)
100%				
	(33.54, 53.21, 354.7°)	(36.94, 57.67, 357.9°)	(40.68, 62.47, 350.5°)	(41.22, 67.59, 346.0°)
50%				
	(33.54, 53.21, 354.7°)	(36.82, 45.43, 357.8°)	(40.54, 50.24, 350.3°)	(41.22, 67.59, 346.0°)




A4.3.2 Effect of uniform colour space based on CIECAM02

In Figure A4-11, the results of adaptive gamut mapping framework performed on CIELAB colour space and uniform colour space based on CIECAM02 are described, respectively. As shown in the figure, the gamut mapping based on uniform colour space shows improved colourfulness especially for the blue colours. To compare the improvement in terms of colour similarity to the original colour, colour patches are picked and the colour difference is calculated in terms of ΔE_{2000} [5]. As shown in the patches and the ΔE_{2000} values, the performance of the gamut mapping could be improved by using uniform colour space. Note that use of uniform colour space improves colour gamut mapping algorithms in general.

FIGURE A4-11

Comparison of adaptive gamut mapping on different colour spaces



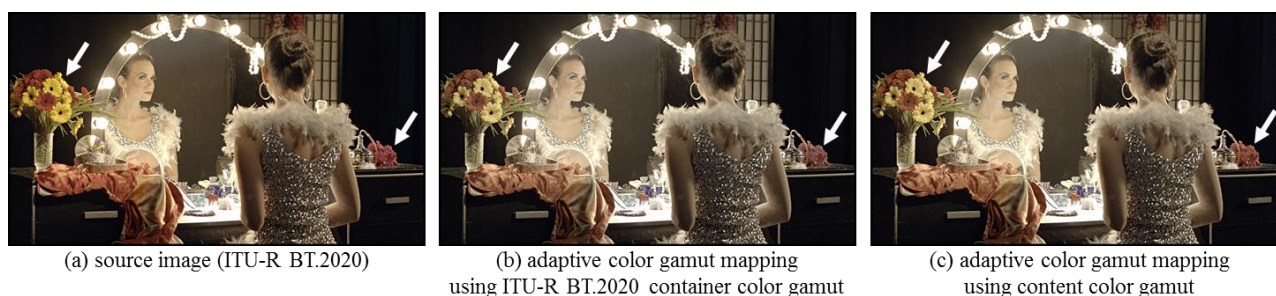
	color patch	$\Delta E_{00}[2:1:1]$
Original		N/A
CIELAB color space		13.9945
Uniform color space based on CIECAM02		9.4761

A4.3.3 Effect of content colour gamut

As the second consideration factor for colour gamut mapping, the effect of content colour gamut is shown in Fig. A4-12. As described in Fig. A4-7, the colour of the original image is distributed in the area smaller than ITU-R BT.2020 container. When a content colour gamut depicted in the Figure is used instead of the container gamut in the adaptive colour gamut mapping framework, the colourfulness is improved as shown in Fig. A4-12(c). Moreover, the colour contrast is also improved since distance between the adjacent colour components is less reduced as the gap between source and target colour gamuts is decreased. Note that use of content colour gamut improves colour gamut mapping algorithms in general.

FIGURE A4-12

Comparison of adaptive colour gamut mapping results without and with content colour gamut



A4.4 Conclusion

In the adaptive gamut mapping framework, preservation of colourfulness as well as the colour contrast is considered. To minimize hue change, the mapping is performed on a constant-hue-angle-plane basis where the hue of source gamut is aligned to the correspondence in the target gamut. The lightness and chroma mapping is performed adaptive to the regions where core region preserves the original colour while the others preserves relative difference between adjacent colour components those are mapped into the target gamut boundary. As shown in the experimental results, the use of core region improves the image quality by preventing loss of details in the saturated colours.

Moreover, two additional factors which improve the gamut mapping result are discussed. From the discussion of the uniform colour space based on CIECAM02, the importance of the uniformity of colour space is stressed. Also, the use of alternative source colour gamut called content colour gamut is studied where it helps to improve colourfulness by reducing the gap between gamut boundaries.

References

- [1] Ján Morovič, *Color Gamut Mapping*, Wiley, 2008.
- [2] M.R. Luo, G. Cui, and B. Rigg, "The development of the CIE 2000 colour-difference formula: CIEDE2000," *Color Research & Application*, vol. 26, no. 5, pp. 340-350, 2001.
- [3] CIE Technical Report 159:2004, "A Colour Appearance Model for Colour Management Systems: CIECAM02," International Commission on Illumination, Vienna, 2004.
- [4] J. Fröhlich, S. Grandinetti, B. Eberhardt, S. Walter, A. Schilling, and H. Brendel, "Creating Cinematic Wide Gamut HDR-Video for the Evaluation of Tone Mapping Operators and HDR-Displays," *SPIE/IS&T Electronic Imaging Conference 2014*, February 5th, 2014.
- [5] ISO/CIE, *Colorimetry-Part 6: CIEDE2000 Colour-difference formula*, ISO/CIE 11664-6:2014. Switzerland: ISO/CIE.

Annex 5

A5.1 Colorimetric colour spaces

In the field of colorimetry, on the other hand, colour spaces have been derived from the properties of the human visual system rather than from display characteristics. An established colour space used to quantify colours visible to the human eye is the system of tristimulus values defined by the Commission Internationale d'Eclairage (CIE) in 1931 [6]. The tristimuli XYZ are related to the aforementioned E_R, E_G, E_B values by the following equations.

$$\begin{bmatrix} X \\ Y \\ Z \end{bmatrix} = \begin{bmatrix} 0.637 & 0.145 & 0.169 \\ 0.263 & 0.678 & 0.059 \\ 0 & 0.028 & 1.061 \end{bmatrix} \begin{bmatrix} R_{2020} \\ G_{2020} \\ B_{2020} \end{bmatrix} = \begin{bmatrix} 0.412 & 0.358 & 0.181 \\ 0.213 & 0.715 & 0.072 \\ 0.019 & 0.119 & 0.951 \end{bmatrix} \begin{bmatrix} R_{709} \\ G_{709} \\ B_{709} \end{bmatrix} \quad (5-1)$$

The tristimulus value Y is referred to as luminance and can be considered an ordinal measure of a colour's perceived brightness, i.e. perceived brightness increases monotonically with luminance but the relationship is not linear. It is important to note that the E_R, E_G, E_B values in equation (5-1) represent linear light signals, either scene referred, as captured by a camera, or display referred, as output by a monitor. The two representations differ by a non-linearity known as the Opto-Optical Transfer Function (OOTF) also known as the rendering intent [1]. Our colour conversion method can be applied to both scene and display referred signals depending on application.

In order to express "colourfulness" independently of luminance, chromaticities x and y are defined by normalising two of the tristimuli:

$$x = \frac{X}{X+Y+Z} \quad \text{and} \quad y = \frac{Y}{X+Y+Z} \quad (5-2)$$

In an attempt to achieve better perceptual uniformity, that is equally perceptible differences across the entire range of colours, a modified set of chromaticities has been defined as part of the CIE 1976 standard [6]:

$$u' = \frac{4X}{X+15Y+3Z} \quad \text{and} \quad v' = \frac{9Y}{X+15Y+3Z} \quad (5-3)$$

Note that u' and v' are linked to x and y by a projective transformation which preserves collinearity, i.e. straight lines in one space remain straight in the other although distance ratios will change between spaces. Projections as used in the following sections can hence be performed equivalently in either space. CIE 1976 $u'v'$ chromaticities throughout this paper will be used.

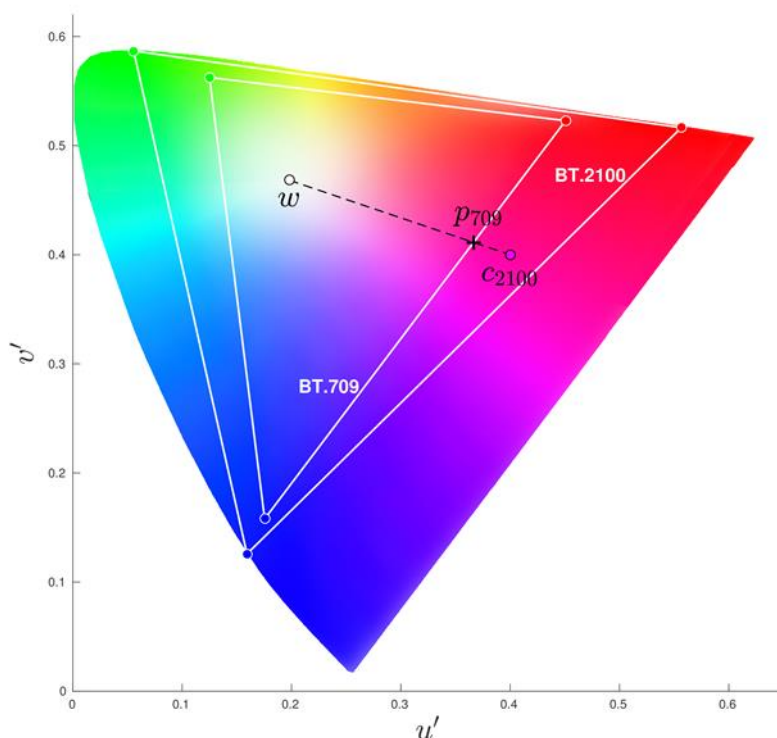
A5.2 Conversion between colour spaces

Mathematically, converting between BT.2020 and BT.709 is a simple change of coordinates that can be achieved by means of equation (5-1). However, in practical systems, E_R, E_G, E_B values represent the relative intensity of each primary's light source (such as an LED) and are thus limited to values between zero and one. As a consequence, the range of physically representable colours, or the gamut, of a colour standard is limited to the triangle spanned by the primaries in chromaticity space. Figure A5-1 shows the gamuts of BT.2020 and BT.709 in comparison to each other. All BT.709 colours also lie in the encompassing BT.2020 gamut; hence they can indeed be up-converted using equation (1), as described in BT.2087 [7].

The remainder of this paper will introduce our approach for going in the opposite direction, namely, for down-converting colours from a wide to a smaller gamut in a meaningful way. While the simplest approach, often taken in practice, is to clip out-of-bound values of R, G and B, this introduces significant, level dependent hue shifts. We attempt to avoid this by desaturating colours appropriately.

FIGURE A5-1

Gamut defined by the primaries of the BT.2020 and BT.709 standards in comparison to the CIE 1976 gamut containing all visible colours



A5.3 Luminance-preserving conversion

A simple, yet effective colour conversion approach is proposed to address the issue that, in real systems, chromaticity and luminance are not independent, a problem which is especially evident at high luminance levels.

In Fig. A5-1, given a source colour with chromaticities $c_{2020} = [u'_{2020}, v'_{2020}]$ outside the BT.709 gamut, the straightforward approach to map c_{2020} to a legal BT.709 colour is by projecting it towards the common white point w onto p_{709} on the BT.709 boundary. This corresponds to a desaturation, which attenuates vivid colours while leaving their hue³ and luminance unchanged.

A5.4 Effective gamut at given luminance

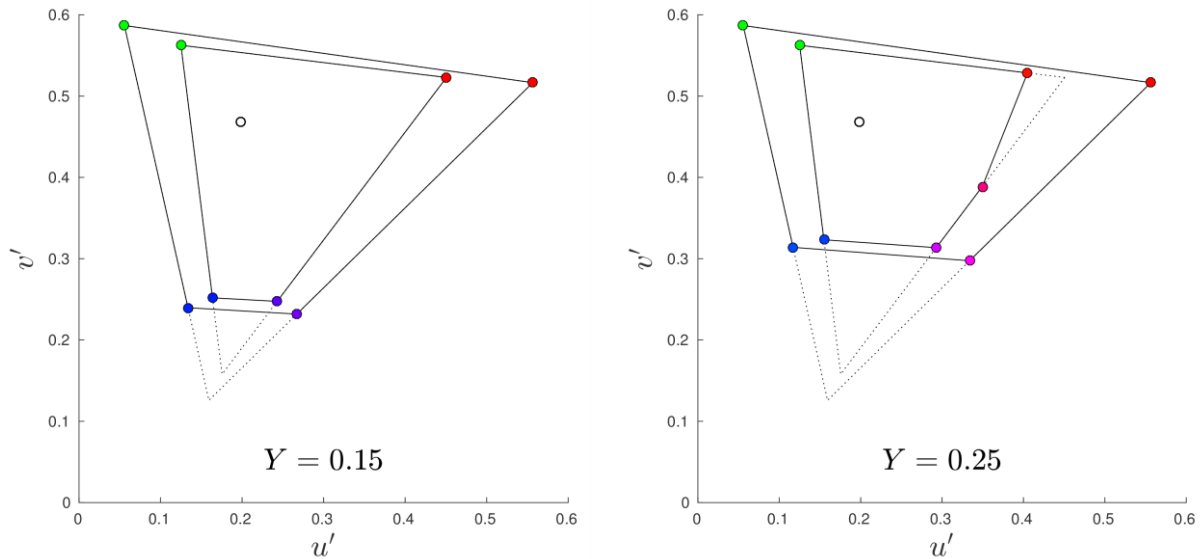
The full gamut, however, is only available for fairly dim colours. As soon as the relative luminance exceeds $Y = 0.059$ for BT.2020 and $Y = 0.072$ for BT.709, the practical gamut that can be achieved (without colour components exceeding one) diminishes. At peak luminance $Y = 1$ only achromatic white is possible.

Figure A5-2 shows the effectively available gamut of both standards for selected luminance values of $Y = 0.15$ and $Y = 0.25$. As can be seen, colours close to the primaries cease to be representable. For both BT.2020 and BT.709, blues are most affected.

³ Since CIE 1931 XYZ space is not perceptually uniform, lines of constant hue are not entirely straight, as recently confirmed in [8]. The resulting hue shifts only become perceptible in extreme cases.

FIGURE A5-2

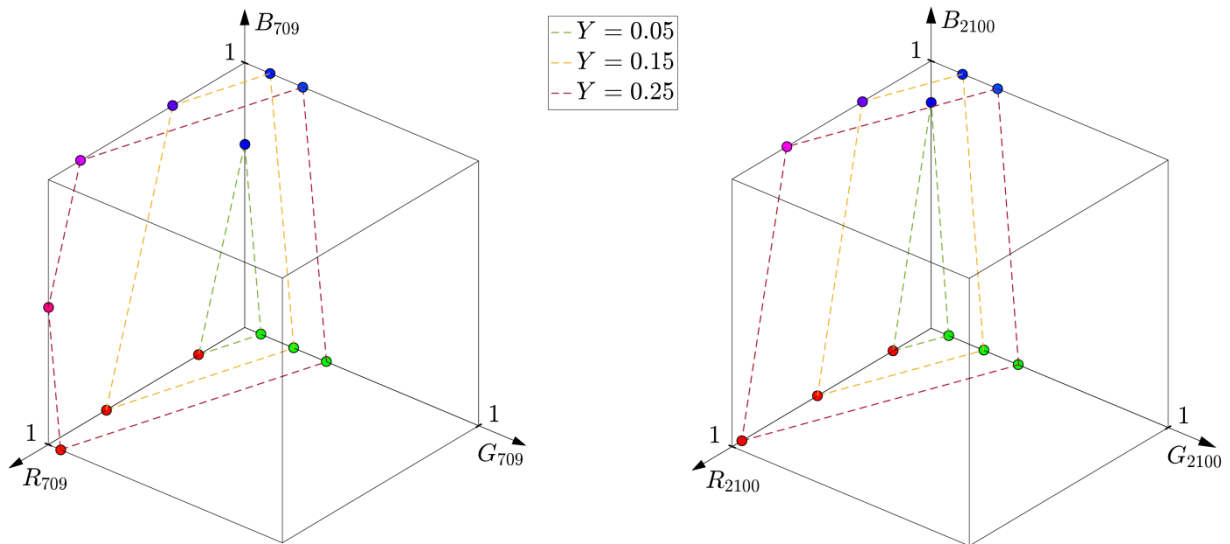
Effective BT.2020 and BT.709 gamuts at different luminance levels



To understand why certain bright colours become unattainable, consider the three-dimensional representation of both colour spaces in Fig. A5-3. The legal range for the R, G, and B components is between zero and one, and all possible colours thus fall inside the so defined cube.

FIGURE A5-3

RGB cubes for BT.709 and BT.2020 with constant luminance planes intersecting them



Colours sharing the same luminance lie on a plane defined by the second rows of equation (5-1), e.g. $Y = 0.213 \cdot R_{709} + 0.715 \cdot G_{709} + 0.072 \cdot B_{709}$, where Y corresponds to the distance of this plane to the origin. For low enough values of Y , the constant-luminance plane intersects the RGB cube in a triangle which, after applying equations (5-2) and (5-3), leads to the typical triangular gamut shown in Fig. A5-1. With increasing Y , the plane moves further and further from the RGB origin and its intersection will skip first the blue, then the red and eventually the green corner of the cube, resulting in a quadrilateral or even pentagonal gamut. For luminance values close to one, the gamut becomes again triangular, albeit “flipped”, i.e. with its corners representing the secondary colours cyan,

magenta and yellow. The three luminance planes plotted in Fig. A5-3 correspond to the gamuts presented in Figs A5-1 and A5-2.

To reflect this effect in our method, instead of using the full target gamut, we propose to project source chromaticities onto the boundary of the effective gamut as defined by the colour's luminance. Performing the projection in either CIE 1931 xy or CIE 1976 $u'v'$ space yields identical results.

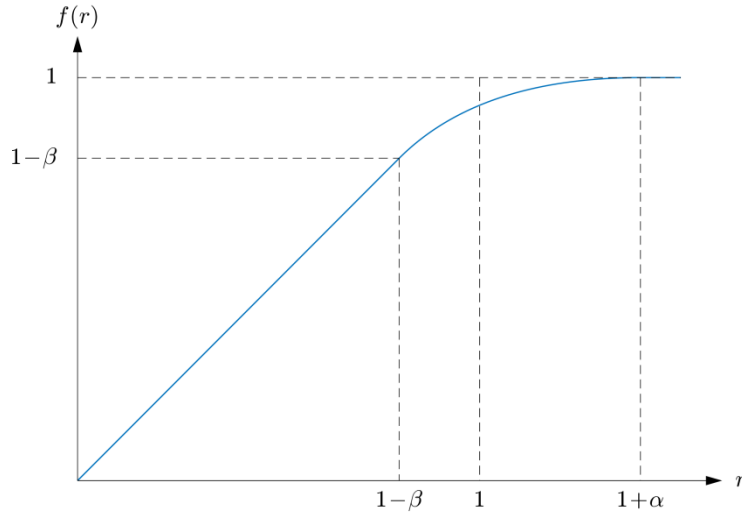
A5.5 Reversible soft-clipping

The projection method described so far is non-reversible. All source colours outside the target gamut that lie on a straight line through the white point are mapped onto the same output colour on the boundary of the effective target gamut. This means that variations in saturation outside the BT.709 gamut are completely lost. As so often in video processing, soft-clipping may capture the original artistic intent better. Soft-clipping preserves at least some of the variation for very bright colours. It also means that the BT.709 colour space may be more accurately expanded back to BT.2020 should this be required.

$$f(r) = \begin{cases} r - \frac{\alpha}{(\beta-\alpha)^2} [\beta - \sqrt{\beta^2 + (\alpha - \beta)(r + \beta - 1)}] & : 1 - \beta < r \leq 1 + \alpha \\ r & : r \leq 1 - \beta \\ 1 & : r > 1 + \alpha \end{cases} \quad (5-4)$$

FIGURE A5-4

Soft-clipping function defined by roll-off parameters α and β



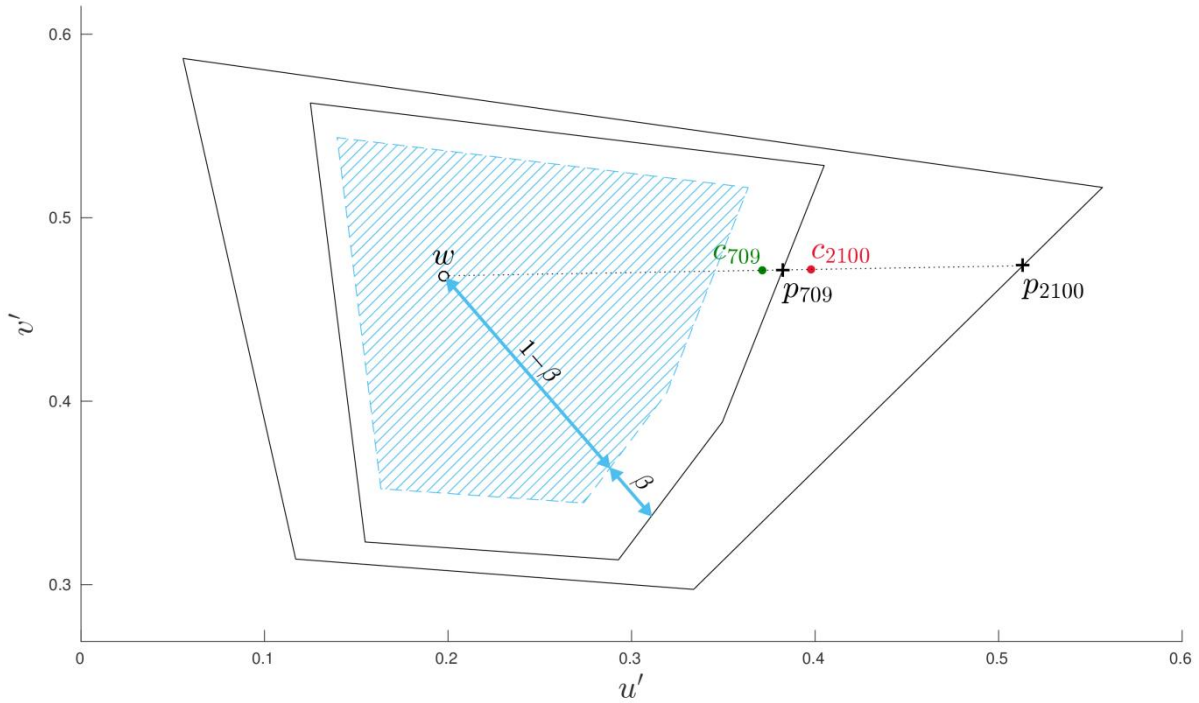
The requirements for the soft-clipping function are that it should smoothly extend the identity function and saturate at one. It is debatable whether the continuation at the high end should be smooth as well as this implies a vanishing derivative and thus infinite compression for high values, which is disadvantageous in terms of reversibility. We have experimented with different functions, including polynomial, exponential, logarithmic and circular arc extensions. For this work, we have chosen a quadratic Bézier curve for its flexibility to control the precise extent of the roll-off region.

The quadratic Bézier extension defined in equation (5-4) is shown in Fig. A5-4. The parameters α and β control the extent of the function's roll-off. More specifically, α will be set such that the boundary of the source gamut maps exactly onto the boundary of the target gamut, and β specifies how much of the target gamut should be sacrificed to accommodate out-of-gamut source colours

(Fig. A5-5). Increasing β facilitates reversibility as the soft-clipping function imposes less compression, but it also reduces the fidelity of colours on the boundary of the target gamut that would otherwise be perfectly representable. Ideally, β should be set as function of the output bit depth, but in this work, we use a fixed value of $\beta = 0.2$.

A5.6 Algorithm

FIGURE A5-5
Mapping of chromaticities between effective gamuts using soft-clipping



The complete algorithm for luminance-preserving colour conversion, including soft-clipping, can be summarised as follows (Fig. A5-5):

1. For input colour, compute luminance⁴ Y and chromaticities⁵ $c_{2020} = [u'_{2020}, v'_{2020}]$
2. Determine effective source and target gamuts at given Y
3. Compute projections p_{2020} and p_{709} onto effective source and target gamuts
4. Set roll-off parameter $\alpha = \overline{w p_{2020}} / \overline{w p_{709}} - 1$
5. Set soft-clipping margin to appropriate value $\beta = 0.2$
6. Compute output chromaticities as $c_{709} = w + \overline{w p_{709}} \cdot f(\overline{w p_{2100}} / \overline{w p_{709}})$
7. Determine output E_R, E_G, E_B values from Y and c_{709}

A source colour c_{2020} outside the target gamut is moved toward the white point w onto c_{709} inside the target gamut. Within the hatched area defined by the distance ratio $(1 - \beta) : \beta$, colours remain unchanged.

⁴ The linear luminance should be calculated either as scene referred or display referred depending on application.

⁵ Working in CIE 1976 $u'v'$ rather than CIE 1931 xy space has the advantage that the effective source and target gamuts are better aligned, and less compression is introduced during soft-clipping.

A5.7 Results

We implemented our approach as a 3D lookup table with $33 \times 33 \times 33$ entries and applied it to a range of display referred linear-light signals from various sources. Results were received as very natural and without noticeable artefacts. For some content, we did, however, notice that extremely saturated bright yellows do suffer from hue shifts, which will require further investigation and improvement of the basic algorithm described here.

A5.8 Conclusion

We have presented a method to convert from a wide-gamut colour space to a colour space with narrower gamut while preserving the luminance of the input. Our approach is reversible in that there is a one-to-one mapping between the input and output colour values. For representations with limited precision, it remains to be investigated how quantisation affects the reversibility in practice. The free soft-clipping parameter of our method will need to be adjusted accordingly.

The results of our approach have been assessed visually and appear to maintain the artistic intent of the source material without noticeable artefacts or major hue changes. Comparative subjective tests are yet to be carried out.

References

- [1] Recommendation ITU-R BT.2100-0 – Image parameter values for high dynamic range television for use in production and international programme exchange, Jul. 2016.
- [2] Devereux, V.G. “Limiting of YUV digital video signals”, BBC R&D White Paper, 1987.
- [3] Recommendation ITU-R BT.601-7, “Studio encoding parameters of digital television for standard 4:3 and wide screen 16:9 aspect ratios,” Mar. 2011.
- [4] Recommendation ITU-R BT.709-6, “Parameter values for the HDTV standards for production and international programme exchange,” June 2015.
- [5] Recommendation ITU-R BT.2020-2, “Parameter values for ultra-high definition television systems for production and international programme exchange,” Oct. 2015.
- [6] CIE 15:2004 Colorimetry, 3rd Edition.
- [7] Recommendation ITU-R BT.2087, “Colour conversion from Recommendation ITU-R BT.709 to Recommendation ITU-R BT.2020,” Oct. 2015.
- [8] Dolby, “ICtCp Dolby White Paper,” <http://www.dolby.com/us/en/technologies/dolby-vision/ICtCp-white-paper.pdf>, retrieved 2016-09-16.

Annex 6

A6.1 Introduction

Annex 6 investigates the possibility of colorimetry conversion from BT.2020 to BT.709 under the requirement of consideration of mastering colour gamut information. The intention is to investigate the possibility of a unique conversion method being able to convert all colours from BT.2020 to BT.709 and at the same time considering the fact that the mastering colour gamut of the content might be smaller than the colour gamut of BT.2020 for some content. In this Annex, a DCI P3 mastering colour gamut is considered as an example. For this reason, BT.2020 content and DCI P3 content

within a BT.2020 container will be considered. Both types of content will be converted by a unique method to BT.709 content as opposed to using a specific mapping for DCI P3 content and another specific method for BT.2020 content. In fact, a specific mapping for DCI P3 content would not be able to handle or would clip colours outside the DCI P3 colour gamut.

The investigated conversion method satisfies the following requirements:

- The conversion method converts full BT.2020 colour gamut into BT.709 colour gamut.
- The conversion method adapts to mastering colour gamut information in order to enhance converted colours for content having been produced within this limited mastering colour gamut.
- The conversion method is static and unique and applies to both, content having full BT.2020 colour gamut and content having limited mastering colour gamut.

The advantages of such a method are:

- Increased saturation after conversion of colours close to BT.2020 colour gamut.
- Increased saturation after conversion of colours close to mastering colour gamut.
- A single conversion method for two types of content.
- The conversion is in principle reversible for both types of content without requiring metadata.

A6.2 Mastering colour gamut information

We understand by mastering colour gamut information the definition of colorimetry of the mastering display that has been used for content production or post-production. Display colorimetry is described by primary colour chromaticity and white point chromaticity. Frequently, mastering colour gamut is DCI P3 such as known from digital cinema production. In this Annex, we investigate colorimetric conversion from BT.2020 to BT.709 for the case of content produced either using BT.2020 colorimetry or P3 colorimetry. However, both types of content are represented using BT.2020 colour coordinates.

A6.3 Conversion method

This Annex investigates a new hue mapping of colours in order to meet the requirements mentioned in the introduction. It is this new hue mapping that makes use of mastering colour gamut information. The new hue mapping is meant to be followed by lightness mapping and chroma mapping such as described in Annex 1 of Annex 7 to Document 6C/158. Hue, lightness and chroma mapping convert the colours from BT.2020 to BT.709. The new hue mapping itself does change the hue of colours as a preparation for lightness and chroma mapping.

The investigated, new hue mapping considers colour gamuts of BT.2020, P3 and BT.709. The colour gamut are each described by their primary and secondary colours in CIELAB space, herein called specific colours. The idea of hue mapping is usually to align hues of specific colours of the source colour gamut (BT.2020) to the corresponding specific colours of the target colour gamut (BT.709). We investigate a new hue mapping that aligns hues of colours dependent on their chroma. The key idea is to align hue of colours with large chroma close to the border to BT.2020 colour gamut differently than colours with smaller chroma. In fact, colours close to the border of the BT.2020 colour gamut are hue mapped guided by how the specific colours of BT.2020 colour gamut are mapped. Therefore, the specific colours of the BT.2020 colour gamut are hue aligned to the corresponding specific colours of the BT.709 colour gamut. Colours with smaller chroma that are close to the border of the mastering colour gamut are hue mapped guided by how the specific colours of the mastering colour gamut are mapped. Therefore, the specific colours of the mastering colour gamut are hue aligned to the corresponding specific colours of the BT.709 colour gamut, too. Colours with even smaller chroma are preferable not hue mapped and preserved.

The investigated, new hue mapping maps BT.2020 colours with same hue in different ways to BT.709 colours that have different hues. The mapping is not hue preserving. The motivation of the new mapping is that the following chroma mapping will be less harmful. In fact, by aligning specific colours of BT.2020 and mastering colour gamuts to BT.709, the content will undergo a more homogeneous chroma mapping, preserving the appearance of smooth colour transitions close to mastering or BT.2020 colour gamut.

For the investigated hue mapping, for each colour to be mapped, an appropriate hue rotation angle in CIELAB space is determined as follows:

1. For all BT.2020 specific colours and corresponding content and target specific colours, a source curve is created going through origin and these three specific colours. Colours lying on the source curve are understood to be source colours from either BT.2020 or P3 content.
2. For all BT.709 specific colours, a straight line, called target line, is defined going through origin and the specific BT.709 colour. Colours lying on the target line are understood to be target colours.
3. For all source curves, for a set of sample source colours lying on the source curve, hue rotation angles are defined such that hue rotation will move a source colour onto a target colour with same chroma lying on the corresponding target line.
4. For any colour to be hue mapped, interpolate a hue rotation angle from the hue rotation angles calculated in last step and apply a hue rotation with this angle to the source colour.

Figure A6-1 shows an example for source curves and target lines for mapping from BT.2020 to BT.709 using P3 colour mastering information. In this example, the source curves have been calculated by a cubic splines.

FIGURE A6-1

Colours on the source curves (continued red line) will be hue rotated onto colours of the corresponding target line (dotted green line), here shown for primary and secondary colours of BT.2020, DCI P3 and BT.709 colour gamut (continued lines) projected into CIE ab plane

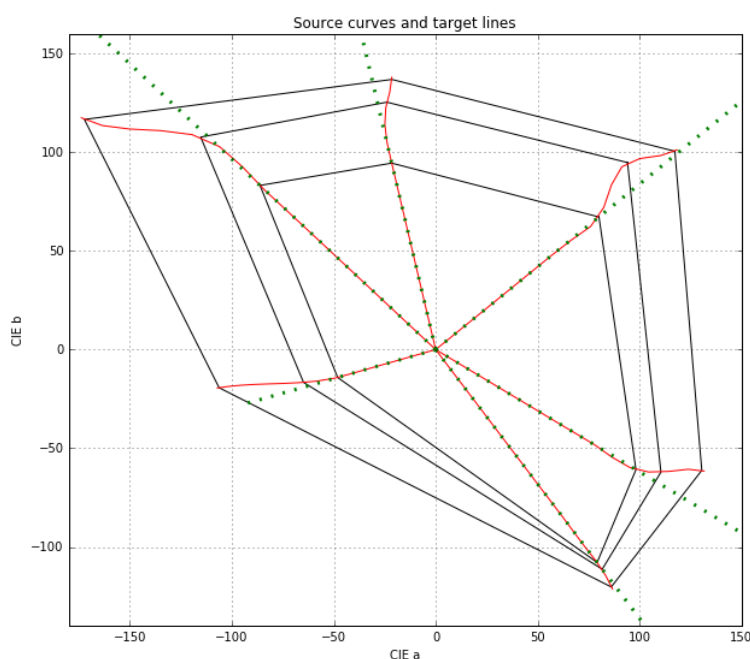


Figure A6-2 shows the hue rotation angles for colours of the sources curves such as calculated in step 3. The angles are calculated in a straight forward manner for a regularly spaced set of colours along the source curves.

Figure A6-3 shows examples of hue rotation angles for any colour from BT.2020 such as calculated in steps 4. In this example, the rotation angles from the colours on the source curves are interpolated using tetrahedral interpolation.

FIGURE A6-2

Values of hue mapping angles shown for colours on the source curves (continued lines starting from the origin) of primary and secondary colours, projected into CIE ab plane, and colour gamuts of BT.2020, DCI P3 and BT.709 (continued, closed lines)

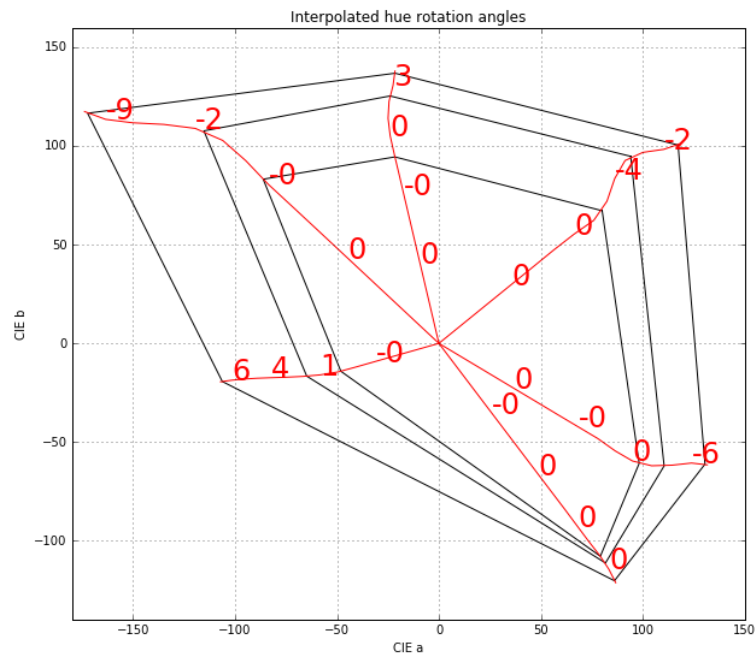
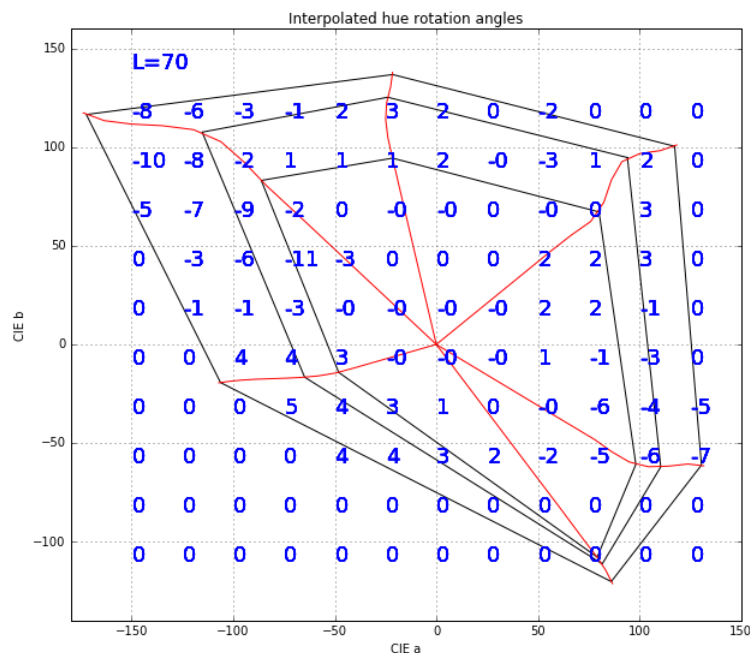


FIGURE A6-3

Hue mapping angles for a sample, regular set of colours at $L=70$, interpolated from the angles such as shown in Fig. A6-2



A6.4 Results

Results in this Annex are produced by modular according to Annex 1 three steps: hue mapping, lightness mapping and chroma mapping.

Three hue mapping methods are compared:

1. No hue mapping: the hue of source colours is preserved in CIELAB space.
2. Classical hue mapping: all colours having the hue of a primary or secondary colour of BT.2020 are mapped to a colour having the hue of the corresponding primary or secondary colour, respectively, of BT.709. The hue of the other colours is linearly interpolated. The hue of all colours is changed.
3. New hue mapping as investigated in this Annex: colours with smaller chroma preserve their hue while colours with larger chroma are hue mapped considering the colours gamuts for BT.2020, BT.709 and the mastering colour gamut.

For all experiments, the lightness mapping and the chroma mapping are identical to the method presented in Annex 1. The hue mapped colours are lightness and chroma mapped in order to fit within the BT.709 colour gamut. The chroma mapping uses straight mapping trajectories in direction to anchor points lying on the lightness axis. Along each mapping trajectory, the colours are compressed using a piece-wise linear compression function that preserves 40% of colours with smaller chroma.

For these experiments, we use the test images shown in Fig. A1-3 (a,b,c,f,g). Figure A6-4 shows the converted test images into BT.709 using (a) the first, (b) the second or (c) the third gamut mapping method, respectively. Line 1 of Fig. A6-4 shows that in spite the non-linear mapping behaviour such as shown in Fig. A6-1, continuity of hues in (1c) is preserved. Line 2 of Fig. A6-4 shows in (2c) notably for red, green and violet that saturation is gained with respect to other hue mapping schemes in (2a, b). This saturation gain is visible too for the red tea box at top right of (3c) and for the red circle on the bottle (5c) and the orange patches at right bottom (5c). Line 4 of Fig. A6-4 shows that the new hue mapping preserves colour differences.

Given results were calculated using display referred linear/nonlinear conversions and narrow range signals.

FIGURE A6-4

Processed test images using (a) no hue mapping or (b) classical hue mapping or (c) new hue mapping

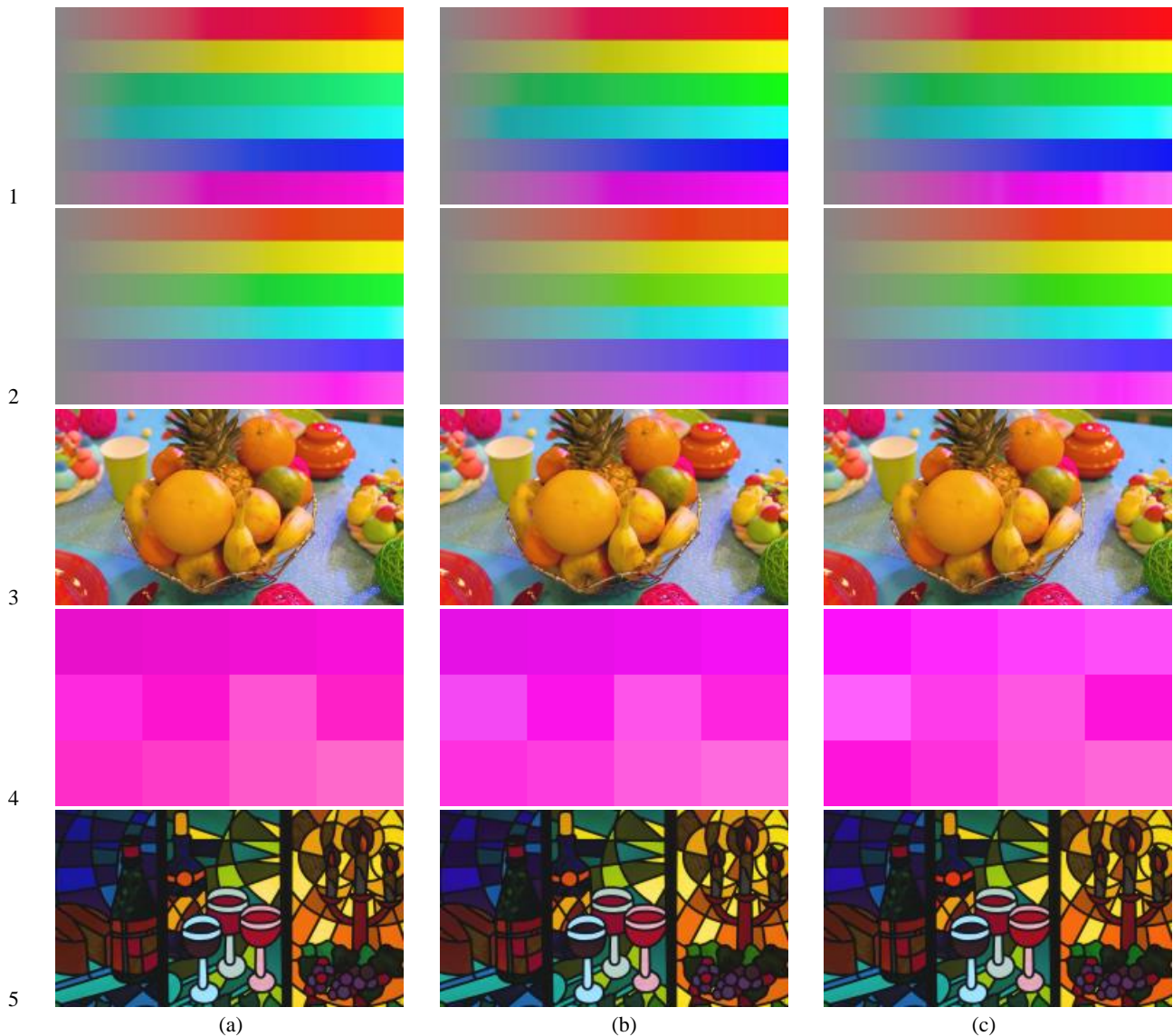
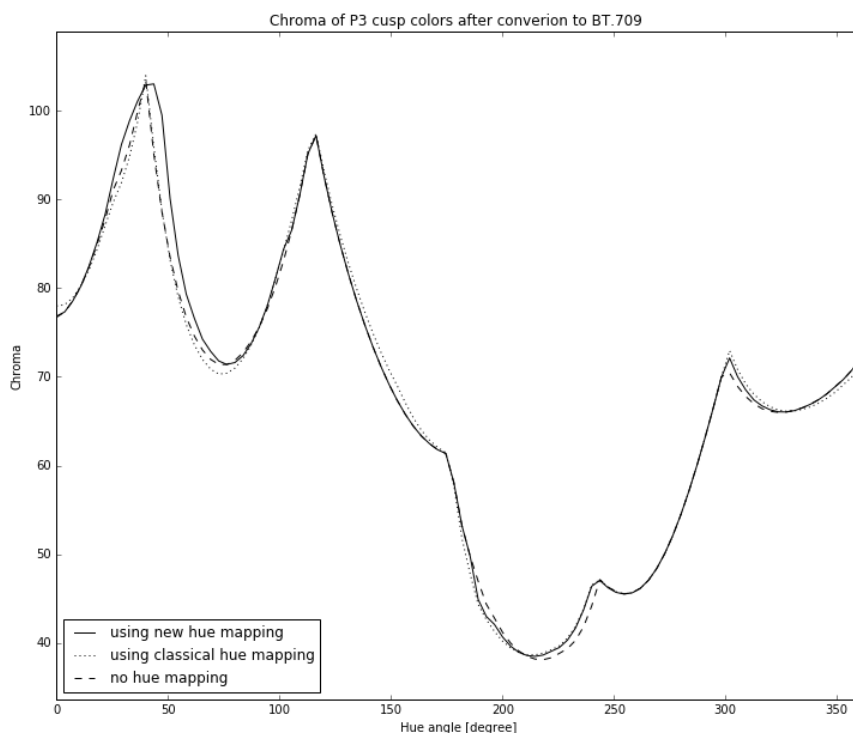


Figure A6-5 shows the chroma of saturated colours on the gamut border of DCI P3 bottom once converted to BT.709. These colours lie regularly on a smooth curve starting at a hue angle of 0° , then passing through red, yellow, green, cyan, blue, violet and ending at a hue angle of 360° . These colours benefits from the investigated hue mapping – notably in the red section – and have a chroma gain as shown in Fig. A6-5.

FIGURE A6-5

Colours close the border of P3 mastering colour gamut for different hue angles once mapped into BT.709 colour gamut using no hue mapping (dashed line), using classical hue mapping (dotted line) and using the new hue mapping (continued line)



A6.5 Conclusions

A new conversion method from BT.2020 to BT.709 is investigated that adapts to mastering colour gamut information. This adaptation is done in specification stage, no metadata is required during operation. The same conversion method is applied to BT.2020 content and to P3 content within a BT.2020 container. Therefore, the method is in principle reversible without requiring metadata. The advantage with respect to known methods is a gain in saturation for colours close to the border of the mastering colour gamut, notably in the red section.